AMAS COURSE ON HIGH PERFORMANCE CEMENT BASED MATERIALS
HPCBM'03 – (PP.135–190) – WARSAW, OCTOBER 16-18, 2003

Test and design method for steel fibre reinforced concrete based on the σ-ε-relation

L. VANDEWALLE

Department of Civil Engineering, K.U.Leuven
3001 Heverlee
Belgium
lucie.vandewalle@bwk.kuleuven.ac.be

Nowadays only a very few design tools are available to analyze the mechanical behaviour of SFRC (steel fibre reinforced concrete) structures. This is due to the fact that primarily the post-peak behaviour is affected by the presence of steel fibres while most design tools used by the structural engineer takes only pre-peak behaviour into account.
Basically there are two possible ways to describe the behaviour of SFRC under tension, especially the non-linear postcracking behaviour: the stress-strain relation (σ-ε) and the stress-crack opening relation (σ-w). These two models have been restraint by RILEM TC162-TDF to set up testing and design methods for SFRC. The σ-ε-design method is based on Eurocode 2 and the design parameters in the σ-ε-relation are determined by means of a displacement controlled bending test on notched prisms. The σ-w-method, however, is derived from the fictitious crack model according to Hillerborg and the direct determination of the $\sigma_w(w)$-relation is done by means of a displacement controlled uni-axial tension test on notched specimens. In this contribution only the σ-ε-design method and companion bending test will be discussed.
Besides also a more fundamental calculation method for crack widths will be presented and compared with test results.

1. Introduction

Since the early seventies, steel fibres are used in concrete to improve its performances. Steel fibres have been proven, mainly by empirical observations, to improve significantly the behaviour of concrete beams and slabs in the serviceability limit state (SLS) by limiting the crack widths and by assuring a more favourable crack distribution.

Promising research results allow also the consideration of using steel fibre reinforced concrete (SFRC) in structural applications (ultimate limit state – ULS) e.g. as shear reinforcement in beams, in tunnel elements, etc. However,

the utilisation of SFRC for structural purposes is quite limited in Europe, mainly due to the lack of National and European Building code requirements for this material.

It is very important to envisage the establishment of a theoretical basis, both for SLS and ULS, in order to allow the design of SFRC-materials for optimum performance. Empirical and semi- empirical design methods bind the designer to certain fibre types and impede a rational optimisation process. In this context, it is very important to realise that current design and test methods for conventionally reinforced concrete structures do not provide such opportunities. This is due to the fact that the "post-peak behaviour (toughness)" is primarily affected by the presence of fibres whilst most design tools used by the structural concrete designer only take pre-peak behaviour (typically Young's modulus and compressive strength) into account. A key requirement for the inclusion of SFRC in future design codes is consequently a well-founded and reliable way to measure and introduce toughness properties of SFRC in the design approach.

To tackle the problems as mentioned above on an international basis a RILEM Technical Committee, i.e. TC162-TDF (Test and Design Methods for Steel Fibre Reinforced Concrete) has been setup in April 1995. Most of the members were already active in standardization with regard to SFRC in their own country.

This contribution reports the work done by this Committee with regard to the σ-ε-design method. Additionally a more fundamental approach with regard to the calculation procedure of crack widths (Dupont [1]) that considers both the interaction between the SFRC and the reinforcement bar and the postcracking tensile strength of the SFRC will be discussed. The RILEM TC162-TDF calculation procedure as well as the more fundamentally based model have been compared with experimental results of 19 full-scale beams.

2. RILEM TC162-TDF – BRITE EURAM project BRPR-CT98-0813

The objectives of TC162-TDF are:

- to develop design methods to accurately evaluate the behaviour of SFRC in structural applications (both in SLS and ULS);
- to make recommendations for appropriate test methods to characterise the (toughness) parameters that are essential in the design methods.

From the beginning it was decided that both items should be treated simultaneously because they are interrelated.

Basically there are two possible ways to describe the behaviour of SFRC under tension, especially the non-linear postcracking behaviour: the stress-strain relation (σ-ε) and the stress-crack opening relation (σ-w) . These two models have been restraint by RILEM TC162-TDF to set up testing and design methods for SFRC. The σ-ε-design method is based on Eurocode 2 and the design parameters in the σ-ε-relation are determined by means of a displacement controlled bending test on notched prisms. The σ-w-method, however, is derived from the fictitious crack model according to Hillerborg and the direct determination of the $\sigma_w(w)$-relation is done by means of a displacement controlled uni-axial tension test on notched specimens.

Consecutively, the Technical Committee consists of two groups, i.e. one group describes the postcracking behaviour of SFRC by means of a stress-strain diagram (σ-ε) and the other by using a stress-crack opening relation (σ-w).

Four "draft recommendations" and two "final recommendations" have been published in "Materials and Structures":

- bending test [2, 3]
- σ-ε-design method [4, 5]
- uni-axial tension test [6]
- σ-w-design method [7].

Between 01.03.1999 and 28.02.2002 the Brite Euram project "Test and Design Methods for Steel Fibre Reinforced Concrete", contract no. BRPR-CT98-0813 has been carried out. The partners in this project were: N.V.Bekaert S.A. (Belgium, co-ordinator), Centre Scientifique et Technique de la Construction (Belgium), Katholieke Universiteit Leuven (Belgium), Technical University of Denmark (Denmark), Balfour Beaty Rail Ltd (Great Britain), University of Wales Cardiff (Great Britain), Fertig-Decken-Union GmbH (Germany), Ruhr-University-Bochum (Germany), Technical University of Braunschweig (Germany), FCC Construction S.A. (Spain), Universitat Politècnica de Catalunya (Spain).

In this project the robustness and repeatibility of both test methods, as proposed by RILEM TC162-TDF, have been thoroughly investigated by means of a round robin study [8]. Some new recommendations to improve these standard tests could be identified and have been discussed in the RILEM Committee. This has resulted in the final recommendation for the bending test, which has been published in Materials and Structures in November 2002 [3].

Consecutively, both design approaches of RILEM TC162-TDF have been checked in the Brite Euram project using an extensive test program, comprising laboratory tests on larger specimens and tests on real structural applica-

tions, the latter in co-operation with the industrial partners. The main topics were bending (SLS and ULS) [9], and shear (ULS) [10]. Some adjustments of the σ-ε-method have been proposed and are taken up in the final recommendation of the σ-ε-design method, which has been published in October 2003 [5].

All reports of the Brite Euram project are collected on a CD-ROM which can be ordered from one of the partners. RILEM Committee TC162-TDF has been closed by the Workshop "Test and Design Methods for Steel Fibre Reinforced Concrete – Background and Experiences", 20-21 March 2003 in Bochum. The workshop gave background information to the recommendations, examples of design and applications [11].

Hereafter, an overview will be given of the latest version of the test and design method based on the σ-ε-relation as proposed by RILEM TC162-TDF.

The objective of the σ-ε-group was to propose a design method which fulfills the following requirements:

- it should be simple enough so that it can be used by a structural engineer for practical applications;
- it should be compatible with the present design regulations for reinforced and prestressed concrete;
- it should make optimum use of the postcracking behaviour of SFRC.

The European pre-standard ENV 1992-1-1 (Eurocode 2: Design of Concrete Structures – Part 1: General rules and rules for buildings) [12] has been used as a general framework for this proposed design method. The calculation guidelines are valid for SFRC with compressive strength of up to C50/60. Steel fibres can also be used in high strength concrete, i.e. concrete with a characteristic cylinder compressive strength $f_{fck} \geq 50\,\text{MPa}$. However, care should then be taken that the steel fibres do not break in a brittle way before being pulled out.

It must be emphasized that these calculation guidelines are intended for cases in which the steel fibres are used for structural purposes and not e.g. for slabs on grade. They also do not apply to other cases such as those in which increased resistance to plastic shrinkage, increased resistance to abrasion or impact, etc. are aimed at.

Since Eurocode 2 takes only the pre-peak behaviour of concrete in tension into account and due to the fact that primarily the post-peak behaviour is affected by the presence of steel fibres, a σ-ε-relation which describes the postcracking behaviour of SFRC has to be developed.

3. Bending test [2, 3]

3.1. Scope

In order to determine the parameters which characterize the postcracking behaviour of SFRC, experimentally, displacement (deflection or crack mouth opening displacement (CMOD)) controlled three-point bending tests are conducted on notched prisms ($150 \times 150 \times 550\,\text{mm}^2$).

This test method evaluates the tensile behaviour of steel fibre-reinforced concrete either in terms of areas under the load-deflection curve or by the load bearing capacity at a certain deflection or crack mouth opening displacement (CMOD). This standard is not intended to be applied in the case of shotcrete. This test method can be used for the determination of:

- the limit of proportionality (LOP), i.e. the stress which corresponds to the point on the load-deflection or load-crack mouth opening displacement curve ($\Rightarrow F_L$) defined in part 3.5 as limit of proportionality;
- two equivalent flexural tensile strengths which identify the material behaviour up to the selected deflection. These equivalent flexural tensile strengths are determined according to part 3.5;
- four residual flexural tensile strengths which identify the material behaviour at a selected deflection or CMOD. The residual flexural tensile strengths are calculated according to procedures in part 3.5.

If the objective of the test is to calculate equivalent flexural tensile strength, it is necessary to measure the deflection. However, if only residual flexural tensile strengths are calculated, one can choose between the measurement of deflection and/or CMOD. A relation between mid span deflection and CMOD is given in 3.6.

The beam specimen is foreseen of a notch, otherwise it is not possible to measure CMOD.

3.2. Test specimen

Concrete beams of 150×150 mm cross section with a minimum length of 550 mm are used as standard test specimens. The standard test specimens are not intended for concrete with steel fibres longer than 60 mm and aggregate larger than 32 mm. The procedure for casting of the specimens and filling of the mould is shown in Fig. 1. It is desirable that portion 1 is twice that of portion 2. The mould shall be filled in one layer up to approximately 90% of the height of the test specimen. The filling procedure of the mould is very important in order to obtain an uniform fibre distribution and the same is certainly true with regard to the compaction procedure. The mould shall

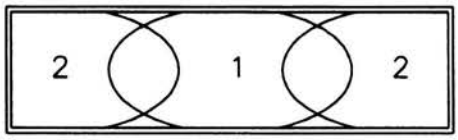

FIGURE 1. Method for filling the mould.

be topped up and levelled off while being compacted. Compaction shall be carried out by external vibration, no internal vibration is allowed. In the case of self-compacting steel fibre concrete, the mould shall be filled in a single pour and levelled off without any compaction.

The specimens are demoulded between 24 and 48 hours after casting the concrete. Afterwards they are stored at +20°C and R.H.$\geq$ 95% until preparation for testing. The beams are notched using wet sawing. Each beam is turned 90° from the casting surface and the notch is then sawn through the width of the beam at mid span (see Fig. 2). Following the notching the same curing conditions for the specimens as before are continued for a minimum of 3 days. The curing can be discontinued not more than 3 hours before testing leaving sufficient time for preparation including any location of measuring devices and transducers. Testing shall normally be performed at 28 days. The width of the notch is not larger than 5 mm and the beam has an unnotched depth h_{sp} of 125 mm$\pm$1 mm. The device for measuring the dimensions of the specimens has an accuracy of 0.1 mm. The dimensions of the specimen shall not vary by more than 2 mm on all sides. Additionally the difference in overall dimensions on opposite sides of the specimen should not be greater than 3 mm.

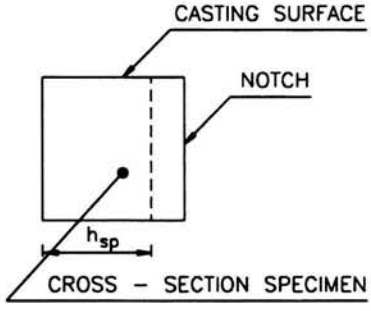

FIGURE 2. Place of the notch.

3.3. Apparatus

A testing machine which is capable of producing a constant rate of increase of deflection (δ) or CMOD of the test specimen, preferably a closed loop machine, should be used. The stiffness of the testing equipment has to be large enough to avoid unstable zones in the F-δ (F-CMOD) curve. Tests during which instabilities occur have to be rejected. The two supports and the device for imposing the displacement are rollers with a diameter of 30 mm±1 mm as shown in Fig. 3. All rollers should be manufactured from steel. Two rollers, including the upper one, should be capable of rotating freely around their axis and of being inclined in a plane perpendicular to the longitudinal axis of the test specimen.

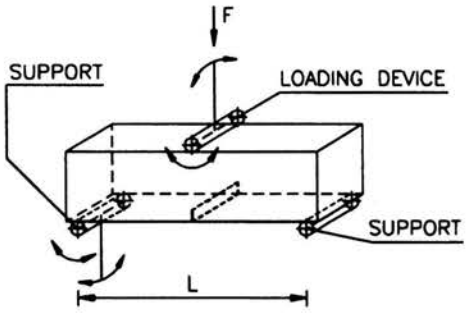

FIGURE 3. Support system.

The apparatus measuring deflection should be capable of recording accurately the mid span deflection, excluding extraneous deformations due to deformations of the machine and/or of the specimen supports. Normally deflection is measured at one side of the specimen ($\Rightarrow \delta$) and the transducer has to be carefully mounted in order to minimise the effect of rotation. A schematic illustration of a possible measuring set-up is shown in Fig. 4. The original distance between the reference points for the measurement of the opening of the mouth of the notch (CMOD) is not greater than 40 mm (Fig. 4). It is recommended that the notch mouth opening displacement measuring system is installed along the longitudinal axis at the mid-width of the test specimen, so that the distance between the bottom of the specimen and the axis of the measuring system is 5 mm or less as explained in 4.4. The accuracy of the load measuring device is required to be equal to 0.1 kN. The accuracy of the deflection and the notch mouth opening displacement measuring system requires to be 0.01 mm.

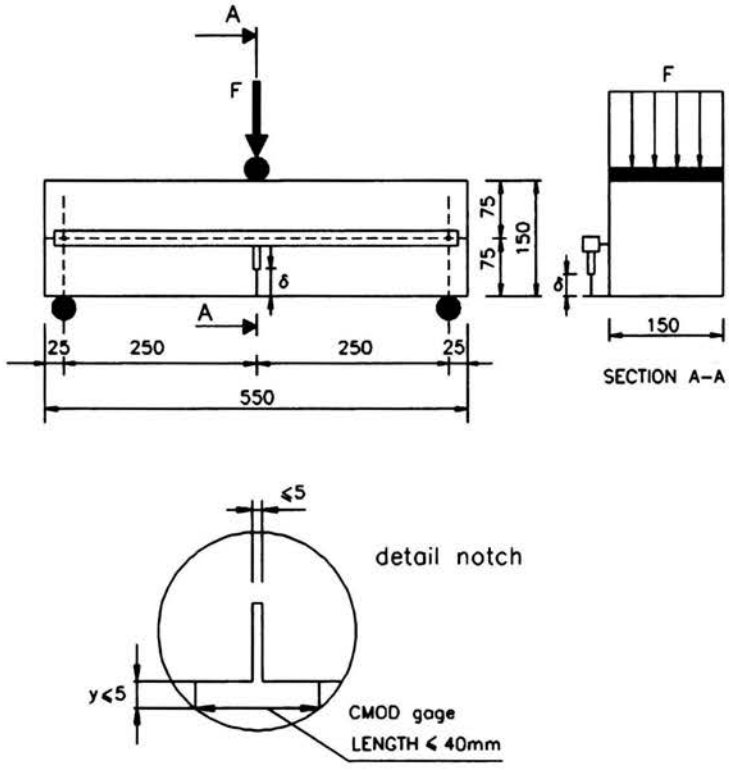

FIGURE 4. Measuring set-up.

3.4. Procedure

The span length of the three-point loading test is 500 mm (Fig. 4). The testing machine should be operated so that the measured deflection of the specimen at mid span increases at a constant rate of 0.2 mm/min until the specified final deflection is reached. During testing the value of the load and deflection at mid span (δ) are recorded continuously. When the test is executed by means of CMOD-control, the machine shall be operated in such a manner that the CMOD increases at a constant rate of 50 μm/min for CMOD from 0 to 0.1 mm, until the end of the test at a constant rate of 0.2 mm/min. During the first two minutes of the test, data shall be logged with a frequency not smaller than 5 Hz; thereafter, up to the end of the test the frequency shall not be smaller than 1 Hz. At least 6 specimens shall be tested in the same conditions.

3.5. Calculation

The load at the limit of proportionality (= F_L in N) is determined according to an appropriate diagram in Fig. 5 or Fig. 6.

F_L is equal to the highest value of the load in the interval (δ or CMOD) of 0.05 mm. The moment at mid span of the test beam corresponding to F_L is:

$$M_L = \frac{F_L}{2} \cdot \frac{L}{2} \quad [\text{Nmm}], \tag{3.1}$$

where L = span of the specimen [mm].

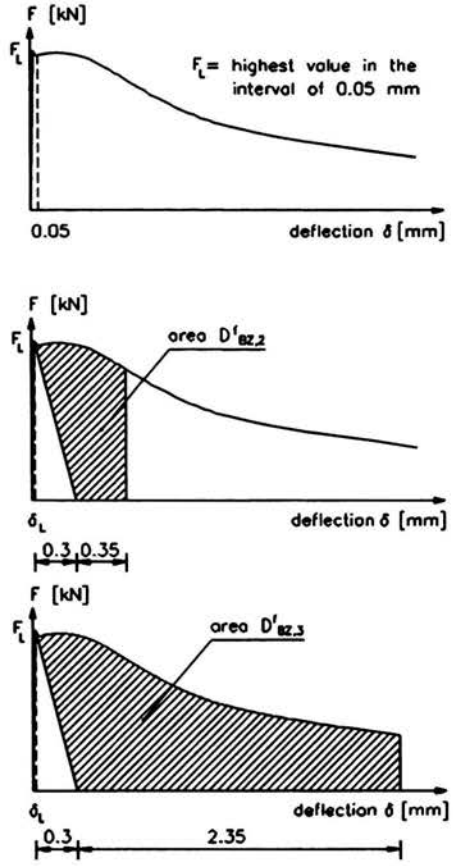

FIGURE 5. Determination of F_L and equivalent tensile strength.

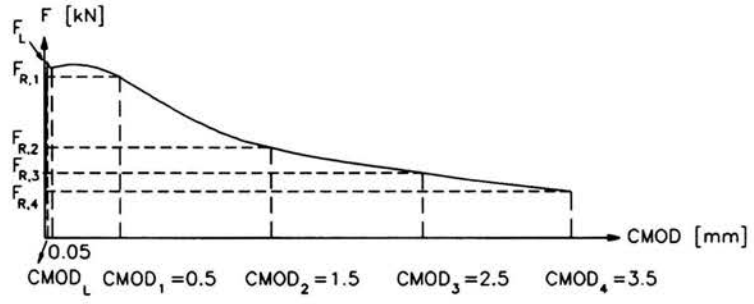

FIGURE 6. Determination of F_L and residual tensile strengths.

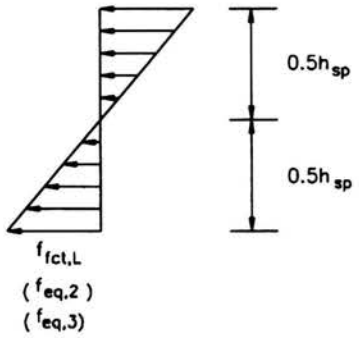

FIGURE 7. Assumed stress distribution for the calculation of $f_{\mathrm{fct,L}}$ and f_{eq} or f_{R}.

Assuming a stress distribution as shown in Fig. 7, the limit of proportionality $f_{\mathrm{fct,L}}$ can be calculated using the following expression:

$$f_{\mathrm{fct,L}} = \frac{3F_L L}{2bh_{\mathrm{sp}}^2} \quad [\mathrm{N/mm^2}], \tag{3.2}$$

where b = width of the specimen [mm], h_{sp} = distance between tip of the notch and top of the cross section [mm].

The energy absorption capacity $D_{\mathrm{BZ},2}$ ($D_{\mathrm{BZ},3}$) is equal to the area under the load-deflection curve up to a deflection $\delta_2(\delta_3)$ (Fig. 5). $D_{\mathrm{BZ},2}(D_{\mathrm{BZ},3})$ consists of two parts:

- plain concrete $\Rightarrow D_{\mathrm{BZ}}^b$ [Nmm],
- influence of steel fibres $\Rightarrow D_{\mathrm{BZ},2}^f$ and $D_{\mathrm{BZ},3}^f$ [Nmm].

The dividing line between the two parts can be simplified as a straight line connecting the point on the curve corresponding to F_L and the point on the abscissa "$\delta_L + 0.3\,\mathrm{mm}$". δ_L is the deflection at the limit of proportionality. The deflections δ_2 and δ_3 are in turn defined as:

- $\delta_2 = \delta_L + 0.65\,\text{mm}$,
- $\delta_3 = \delta_L + 2.65\,\text{mm}$.

$F_2(F_3)$ is equal to the mean force recorded in the shaded area $D^f_{\text{BZ},2}(D^f_{\text{BZ},3})$ and can be calculated as follows:

$$F_2 = \frac{D^f_{BZ,2}}{0.50} \quad [\text{N}], \tag{3.3}$$

$$F_3 = \frac{D^f_{\text{BZ},3}}{2.5} \quad [\text{N}]. \tag{3.4}$$

The moment at mid span of the test beam corresponding to $F_2(F_3)$ is:

$$M_2 = \frac{F_2}{2}\frac{L}{2} = \frac{D^f_{\text{BZ},2}}{0.50}\frac{L}{4} \quad [\text{Nmm}], \tag{3.5}$$

$$M_3 = \frac{F_3}{2}\frac{L}{2} = \frac{D^f_{\text{BZ},3}}{2.5}\frac{L}{4} \quad [\text{Nmm}]. \tag{3.6}$$

Assuming a stress distribution as shown in Fig. 7, the equivalent flexural tensile strength $f_{\text{eq},2}$ and $f_{\text{eq},3}$ can be determined by means of the following expressions:

$$f_{\text{eq},2} = \frac{3}{2}\frac{D^f_{\text{BZ},2}}{0.50}\frac{L}{bh^2_{\text{sp}}} \quad [\text{N/mm}^2], \tag{3.7}$$

$$f_{\text{eq},3} = \frac{3}{2}\frac{D^f_{\text{BZ},3}}{2.5}\frac{L}{bh^2_{\text{sp}}} \quad [\text{N/mm}^2]. \tag{3.8}$$

The postcracking parameters of SFRC which are used in the σ-ε-design method are the residual flexural tensile strengths $f_{\text{R,i}}$. They can be calculated either from a load-deflection curve or from a load-CMOD-diagram since there exists a correlation between deflection and CMOD as explained in (3.6) and (4.4).

Residual flexural tensile strengths $f_{\text{R,i}}$ at the following mid span deflections ($\delta_{\text{R,i}}$) or crack mouth opening displacements (CMOD_i) can be calculated:

$$\delta_{\text{R},1} = 0.46\,\text{mm} - \text{CMOD}_1 = 0.5\,\text{mm},$$
$$\delta_{\text{R},2} = 1.31\,\text{mm} - \text{CMOD}_2 = 1.5\,\text{mm},$$

$$\delta_{R,3} = 2.15\,\text{mm} - \text{CMOD}_3 = 2.5\,\text{mm},$$
$$\delta_{R,4} = 3.00\,\text{mm} - \text{CMOD}_4 = 3.5\,\text{mm}.$$

$F_{R,i}$ is the load recorded at $\delta_{R,i}$ or CMOD_i. Assuming a stress distribution as shown in Fig. 7, the residual flexural tensile strength $f_{R,i}$ can be determined by means of the following expression:

$$f_{R,i} = \frac{3}{2}\frac{F_{R,i}L}{bh_{sp}^2} \quad [\text{N/mm}^2]. \tag{3.9}$$

Note: if the crack starts outside the notch, the test has to be rejected.

3.6. Equivalence between δ and CMOD

The following average relationship between CMOD and δ was determined:

$$\text{CMOD} = 1.18\delta + \beta \text{ with } \beta = -0.0416\,\text{mm}.$$

It must be stressed that this relationship is only applicable in the post-peak region of the load-CMOD (load-δ) curve. The beam response at CMOD 0.5 mm, 1.5 mm, 2.5 mm and 3.5 mm is of special interest. The corresponding values of δ were mentioned before. In the case where CMOD is measured at a certain distance y (see Fig. 4) below the beam, resulting in a measurement CMOD_y, the following relationship between CMOD and CMOD_y can be adopted:

$$\text{CMOD}_y = \text{CMOD}\frac{H+y}{H} \quad [\text{mm}], \tag{3.10}$$

with H = total heigth of the beam.

More explanation will be given in 4.4.

4. Round robin analysis of the bending test [8,13-15]

4.1. Test programme

The test programme included both plain and steel fibre reinforced concrete beams. The material variables for the SFRC beams consisted of two concrete strengths (C25/30 – normal strength concrete (NSC) / C70/85 – high strength concrete (HSC)), three fibre dosages (25, 50 and 75 kg/m^3) and three types of fibres (Dramix 80/60 BN, 65/60 BN and 80/60 BP). The plain concrete beams essentially play the role of control specimens and were a means of investigating the strengths, limitations and sensitivity of the proposed test method, as they do not contain variations introduced by fibre distribution and orientation.

Five laboratories were involved in the round robin programme:

- Belgian Building Research Institute
- Technical University of Denmark
- Katholieke Universiteit Leuven
- Ruhr-University of Bochum
- Cardiff University (Task co-ordinator).

The round robin test programme was divided into two phases. The main objective of the first phase was to investigate the strength and limitations of the RILEM proposed beam test. Table 1 presents details of the test programme.

TABLE 1. Overall round robin test programme.

Testing lab	Number of specimens					
	First phase		Second phase			
	C25/30		C25/30		C70/85	
	0 kg/m^3	50[1] kg/m^3	25[2] kg/m^3	75[2] kg/m^3	0 kg/m^3	25[3] kg/m^3
1	8	8	6	6	6	6
2	8	8	6	6	6	6
3	8	8	6	6	6	6
4	8	8	6	6	6	6
5	8	8	6	6	6	6
Total	40	40	30	30	30	30

Superscript 1 indicates Dramix 80/60BN(*) was used

Superscript 2 indicates Dramix 65/60 BN was used

Superscript 3 indicates Dramix 80/60 BP was used

(*) 80: aspect ratio of the fibre (length/diameter = L/N)
60: length of fibre (L in mm)
B: no coating
N: low carbon, i.e. minimum yield strength of 1100 MPa
P: high carbon, i.e. minimum yield strength of 2500 MPa.

4.2. Results

Figures 8 and 9 present typical P-δ and P-CMOD curves for the plain NSC and HSC beams. Figures 10 and 11 show the corresponding results for the SFRC beams specimens.

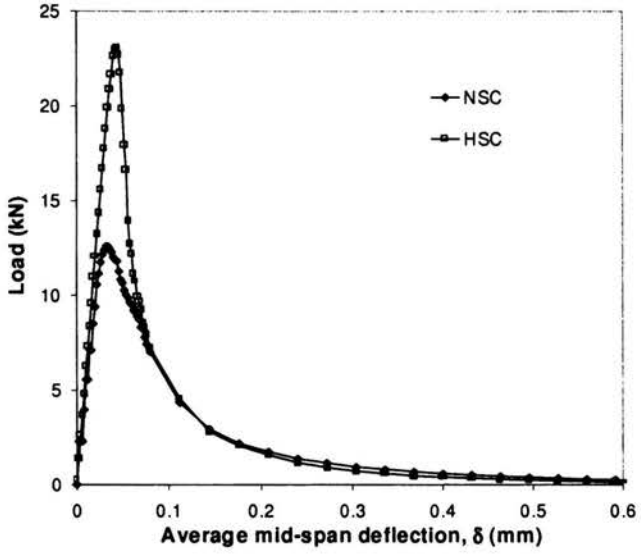

FIGURE 8. Typical P-δ-curves for plain concrete.

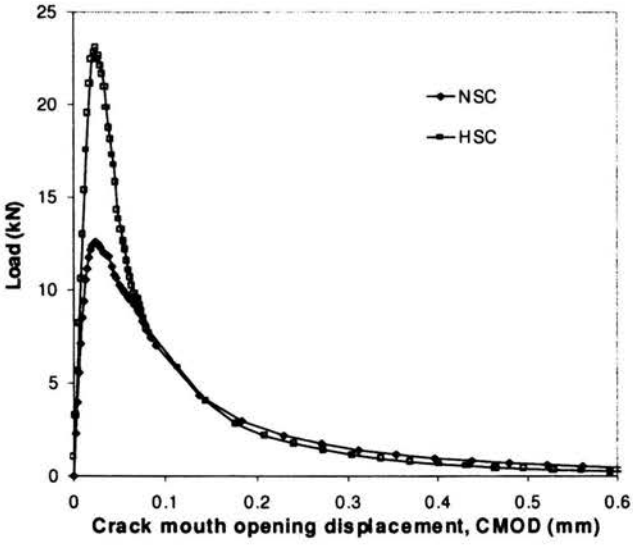

FIGURE 9. Typical P-CMOD curves for plain concrete.

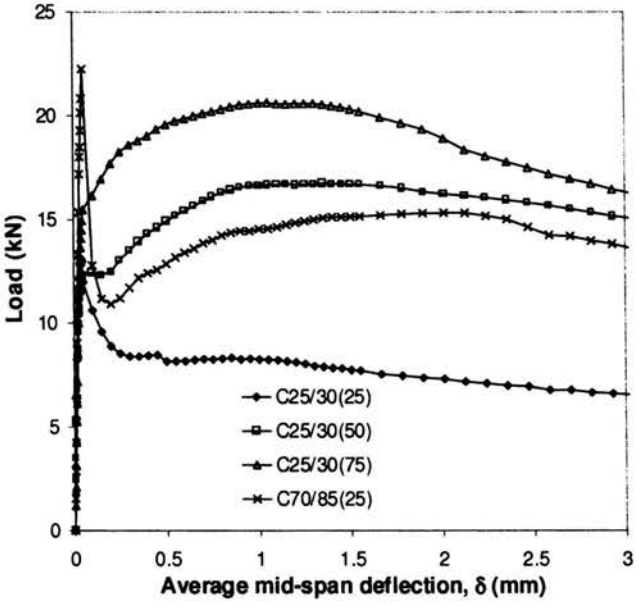

FIGURE 10. Typical P-δ-curves for SFRC.

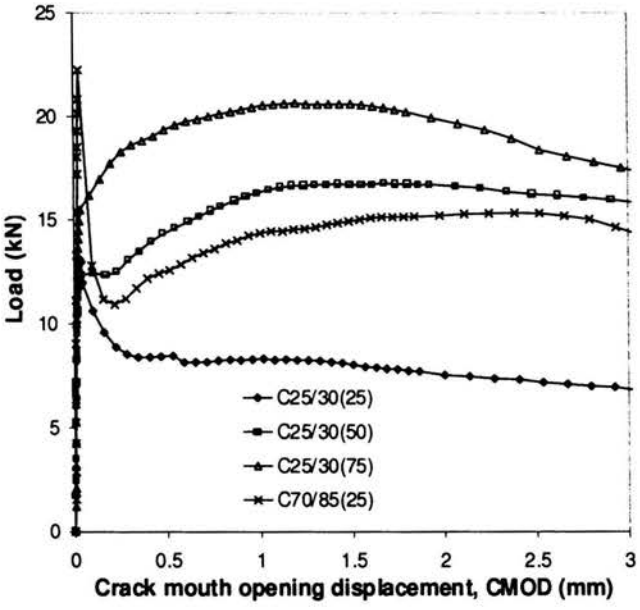

FIGURE 11. Typical P-CMOD curves for SFRC.

4.3. Evaluation of the bending test

The round robin test programme showed that the three-point bending test on a notched prism is a good robust test which is relatively easy to carry out. In particular, the test boundary conditions are able to adapt and tolerate surface non-uniformity in the test specimens. The test specimens are sufficiently large to allow a range of fibre sizes and fibre dosages to be tested as part of development work with new fibres or as control test specimens. Care should be taken to avoid improper or/and excessive vibration, as it would lead to undesirable fibre orientation.

The main limitation of the beam test is that it is not suitable for testing shotcrete and concrete in existing structures.

It has been shown that the load-CMOD curve (rather than the load-deflection curve) can be used to calculate the proposed Rilem design parameters, i.e. residual strengths at predetermined CMODs (or deflections δ): $f_{R,1}$: CMOD = 0.5 mm – $f_{R,4}$: CMOD = 3.5 mm. The calculation procedure to obtain the residual strengths is very short and simple to carry out. The procedure for calculating the equivalent flexural tensile strengths, $f_{eq,2}$ and $f_{eq,3}$, however, is quite lengthy and relatively difficult to carry out.

The notch has the advantage that it allows CMOD to be used to control the test itself. This is significant in the case of low fibre dosages and/or high strength concrete mixes since the bending test is much more stable with CMOD-control than with δ-control.

A detailed analysis of both intra-lab, inter-lab and within-mixes results showed that although inter-lab variations do occur, this was relatively small compared to the inherent material variation which is the dominating factor resulting in relatively high coefficients of variation observed in the round robin test programme. This variation was greatest at the lowest fibre dosage (25 kg/m^3, variation from 15 to 25%) and decreased as the fibre dosage increased (75 kg/m^3, 10 to 20%). This is due to the difficulty in achieving a uniform fibre distribution especially with low fibre contents. A fibre count showed that the toughness parameters were directly related to the number of fibres intersecting the fracture surface. Another possible reason for the high variation is that the specimens have relatively small cross sections. A small variation or difference in number of fibres has a direct and relatively large influence on the toughness of the material tested. This phenomenon would be more pronounced in specimens with lower fibre dosages. Finally, since compaction of SFRC mixes inevitably leads to a degree of fibre orientation (which more often than not is advantageous) care needs to be exercised to ensure that the preparation of the beam specimens is similar to that of the real structure.

In the draft recommendation of the bending test the mid span deflection had to be measured on both sides of the beam (referred to as δ_1 and δ_2). A systematic fibre counting exercise was carried out on several beam specimens to investigate whether there is a correlation between differences between δ_1 and δ_2 and the fibre distribution. The findings of the investigation suggest that differences between δ_1 and δ_2 are not strongly linked with the fibre distribution regardless of concrete strength. It is likely that this phenomenon arises because the supports and loading points have enough degrees of freedom to accommodate any unevenness of the specimen surface. This reflects well on the robustness of the proposed test method as it means that the proposed boundary conditions are able to adapt and tolerate (to a certain degree) surface uniformity. However, it is also suggested that significant differences between δ_1 and δ_2 may be brought about by experimental errors.

In the final version of the bending test, the deflection has only to be measured at one side of the beam specimen.

Additionally, an investigation was carried out to evaluate the objectiveness of the calculation procedure proposed by RILEM TC162-TDF to obtain the necessary design parameters. It was found that the prescribed calculation procedure was satisfactory, as the variation between the design parameters calculated at different laboratories was generally within the range of $\pm$ 5%.

4.4. Relationship between δ and CMOD

A detailed analysis was carried out to investigate the influence of different test configurations on measurements of CMOD. Linear elastic fracture mechanics (LEFM) and non-linear fracture mechanics methods (NLFM) were utilised to investigate the problem analytically. From the analytical studies carried out, it is proposed by the consortium of the Brite Euram project that the CMOD should not be measured at a distance ($= y$) more than 5 mm from the bottom fibre of the beam as shown in Fig. 4. A larger distance than 5 mm will cause the deviation between the measured CMOD_y and the true CMOD to reach an unacceptable level.

In the postcracked phase, it can be shown by comparing the NLFM analysis and experimental results that the average mid span deflection δ can be related to CMOD using the simple rigid body model shown in Fig. 12.

The relation δ to CMOD_y is as follows:

$$\frac{\delta}{\text{CMOD}_y} = \frac{L}{4}\frac{1}{d}, \tag{4.1}$$

where L = span of the beam [mm], d = the apparent depth about which the beam rotates [mm].

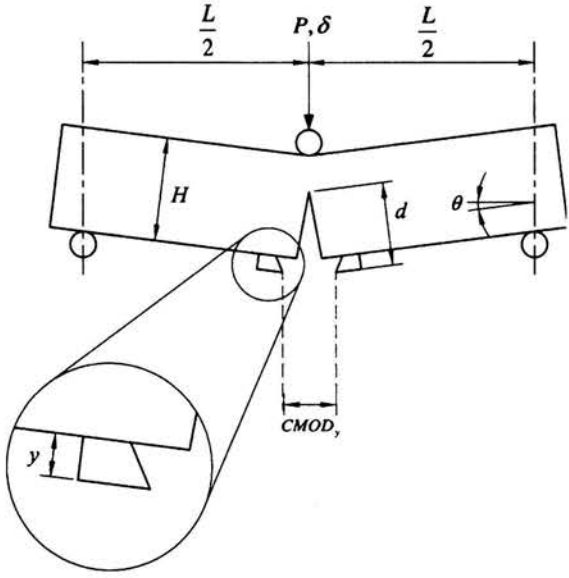

FIGURE 12. Rigid body model of the beam test.

The only problem is to evaluate the value of d, i.e. the crack length. In the postcracked phase it can be assumed that the point at which the beam rotates is situated at the very top surface of the beam. Apart from using the experimental results for the verification of equation (4.1), a computer program developed at the Technical University of Denmark, DTU, was used in addition to the simple proposed model. A series of different material behaviours was investigated resulting in a series of slightly different CMOD-δ-relationships. The final, universal relationship between CMOD and δ is based on an averaging of the different relationships, that means that this relationship is independent of the fibre content and of the concrete strength:

$$\text{CMOD} = 1.18\delta + \beta \text{ with } \beta = -0.0416\,\text{mm}.$$

Analysis with regard to the accuracy of the proposed rigid body model was carried out using both experimental and analytical results. In both plain and especially for SFRC beams, it was found that there was close agreement between the model and the experimental and analytical results. The conversion from CMOD to the equivalent mid span deflection δ_e, revealed good agreement between the load-average mid-span deflection (F-δ) curve and load-equivalent mid-span deflection (δ_e) curve.

5. σ-ε-design method [16]

5.1. Material properties

5.1.1. Compressive strength. The compressive strength of steel fibre reinforced concrete (= SFR-concrete) should be determined by means of standard tests, either on concrete cylinders ($\Phi = 150\,\text{mm}$, $h = 300\,\text{mm}$) or concrete cubes (side = 150 mm). The design principles are based on the characteristic 28-day strength, defined as that value of strength below which no more than 5% of the population of all possible strength determinations of the volume of the concrete under consideration, are expected to fall. Hardened SFR-concrete is classified in respect to its compressive strength by SFR-concrete strength classes which relate to the cylinder strength f_{fck} or the cube strength $f_{fck,cube}$ (Table 2). Those strength classes are the same as for plain concrete.

TABLE 2. Steel fibre reinforced concrete strength classes: characteristic compressive strength f_{fck} (cylinders), mean $f_{fctm,fl}$ and characteristic $f_{fctk,fl}$ flexural tensile strength in N/mm^2; mean secant modulus of elasticity in kN/mm^2.

Strength class of SFRC	C20/25	C25/30	C30/37	C35/45	C40/50	C45/55	C50/60
f_{fck}	20	25	30	35	40	45	50
$f_{fctm,fl}$	3.7	4.3	4.8	5.3	5.8	6.3	6.8
$f_{fctk,fl}$	2.6	3.0	3.4	3.7	4.1	4.4	4.8
E_{fcm}	29	30.5	32	33.5	35	36	37

5.1.2. Flexural tensile strength. When only the compressive strength f_{fck} has been determined, the estimated mean and characteristic flexural tensile strength of steel fibre reinforced concrete may be derived from the following equations:

$$f_{fctm,ax} = 0.3 \cdot (f_{fck})^{2/3} \quad [N/mm^2], \tag{5.1}$$

$$f_{fctk,ax} = 0.7 \cdot f_{fctm,ax} \quad [N/mm^2], \tag{5.2}$$

$$f_{fct,ax} = 0.6 \cdot f_{fct,fl} \quad [N/mm^2], \tag{5.3}$$

$$f_{fctk,fl} = 0.7 \cdot f_{fctm,fl} \quad [N/mm^2]. \tag{5.4}$$

The corresponding mean and characteristic values for the different steel fibre reinforced concrete strength classes are given in Table 2.

If bending tests are performed, the following method [17] can be used to determine the characteristic value of the limit of proportionality (LOP)

(cfr. bending test) [3]:

$$f_{\mathrm{fctk,L}} = f_{\mathrm{fctm,L}} - k_{\mathrm{x}} s_{\mathrm{p}} \quad [\mathrm{N/mm^2}], \tag{5.5}$$

with $f_{\mathrm{fctk,L}}$: characteristic value of LOP [N/mm^2], $f_{\mathrm{fctm,L}}$: mean value of LOP [N/mm^2], s_{p}: standard deviation [N/mm^2],

$$s_{\mathrm{p}} = \sqrt{\frac{\sum (f_{\mathrm{fctm,L}} - f_{\mathrm{fct,L}})^2}{(n-1)}}, \tag{5.6}$$

n: number of specimens, k_{x}: factor dependent on the number of specimens; some values are given in Table 3.

The maximum value of expression (5.4) and (5.5) can be taken as the flexural tensile strength of the SFR-concrete.

TABLE 3.

N	1	2	3	4	5	6	8	10	20	30	4
k_{xknown}	2.31	2.01	1.89	1.83	1.80	1.77	1.74	1.72	1.68	1.67	1.64
k_{xunknown}	–	–	3.37	2.63	2.33	2.18	2.00	1.92	1.76	1.73	1.64

In Table 3, k_{xunknown} means that the coefficient of variation of the population is unknown; instead of the standard deviation of the population, the standard deviation of the spot check will be used.

The mean value of the secant modulus E_{fcm} in kN/mm^2 is also given in Table 2.

5.1.3. Residual flexural tensile strength The residual flexural tensile strength $f_{\mathrm{R,i}}$, which is an important parameter characterising the postcracking behaviour of steel fibre reinforced concrete, is determined by the CMOD (crack mouth opening displacement) – or deflection controlled bending test [3]. The residual flexural tensile strengths $f_{\mathrm{R,1}}$, $f_{\mathrm{R,4}}$ respectively, are defined at the following crack mouth opening displacement (CMOD_i) or mid span deflections ($\delta_{R,i}$):

$$\mathrm{CMOD}_1 = 0.5\,\mathrm{mm} - \delta_{R,1} = 0.46\,\mathrm{mm},$$
$$\mathrm{CMOD}_4 = 3.5\,\mathrm{mm} - \delta_{R,4} = 3.00\,\mathrm{mm},$$

and can be determined by means of the following expression:

$$f_{\mathrm{R,i}} = \frac{3F_{\mathrm{R,i}}L}{2bh_{\mathrm{sp}}^2} \quad [\mathrm{N/mm^2}], \tag{5.7}$$

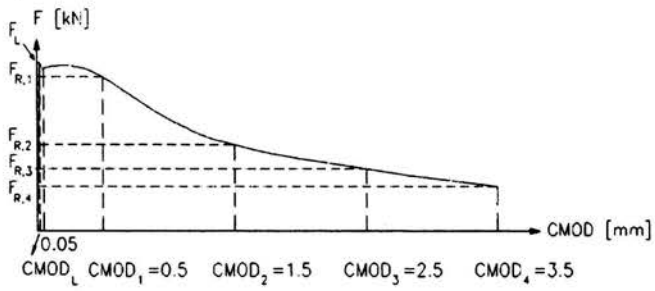

FIGURE 13. Load – CMOD diagram.

where b = width of the specimen [mm], h_{sp} = distance between tip of the notch and top of cross section [mm], L = span of the specimen [mm], $F_{R,i}$ = load recorded at $CMOD_i$ or $\delta_{R,i}$ [N] (see Fig. 13).

The relation between "characteristic" and "mean" residual flexural tensile strength is given in 5.1.2 (Eq. (5.5)).

Hardened SFR-concrete is classified by using two parameters that are determined by the residual flexural strengths $f_{R,1}$ and $f_{R,4}$. The first parameter $FL_{0.5}$ is given by the value of $f_{R,1}$ reduced to the nearest multiple of 0.5 MPa, and can vary between 1 and 6 MPa. The second parameter $FL_{3.5}$ is given by the value of $f_{R,4}$ reduced to the nearest multiple of 0.5 MPa, and can vary between 0 and 4 MPa. These two parameters denote the minimum guaranteed characteristic residual strengths at CMOD values of 0.5 and 3.5 mm, respectively. The residual strength class is represented as $FL\ FL_{0.5}/FL_{3.5}$, with the corresponding values of the two parameters. For example, a SFRC with a characteristic cylinder compressive strength of 30 MPa, and $f_{R,1} = 2.2$ MPa and $f_{R,4} = 1.5$ MPa would have $FL_{0.5} = 2.0$ MPa and $FL_{3.5} = 1.5$ MPa and be classified as C30/37 F_L 2.0/1.5.

5.2. Design at ultimate limit states: bending and axial force

5.2.1. General. The design method was originally developed without size-dependent safety factors. A comparison of the predictions of the design method and of the experimental results of structural elements of various sizes revealed a severe overestimation of the carrying capacity by the design method. In order to compensate this effect, size-dependent safety factors have been introduced. It should be outlined that the origin of this apparent size-effect is not yet fully understood. Further investigation is required in order to identify if it is due to a discrepancy of material properties between different batches, to a size-effect intrinsic to the method, or a combination of both.

In assessing the ultimate resistance of a cross section, the assumptions given below are used:

- plane sections remain plane (Bernoulli hypothesis);
- the stresses in the steel fibre reinforced concrete in tension as well as in compression are derived from the stress-strain diagram shown in Fig. 14 and explained after Fig. 15;
- the stresses in the reinforcement (bars) are derived from an idealised bi-linear stress-strain diagram;
- for cross sections subjected to pure axial compression, the compressive strain in the SFR-concrete is limited to -2‰. For cross sections not fully in compression, the limiting compressive strain is taken as -3.5‰. In intermediate situations, the strain diagram is defined by assuming that the strain is -2‰ at a level $\frac{3}{7}$ of the height of the compressed zone, measured from the most compressed face;
- for steel fibre reinforced concrete which is additionally reinforced with bars, the strain is limited to 25‰ at the position of the reinforcement (Fig. 15);
- to ensure enough anchorage capacity for the steel fibres, the maximum deformation in the ultimate limit state is restricted to 3.5 mm. If crack widths larger than 3.5 mm are used, the residual flexural tensile strength corresponding to that crack width and measured during the bending test has to be used to calculate σ_3. It is recommended that this value, which replaces $f_{R,4}$, should not be lower than $1\,N/mm^2$;
- in some cases, as mentioned below, the contribution of the steel fibres near the surface has to be reduced. For this reason the steel fibres should not be taken into account in a layer near the surface:

  for exposure class 2 [12]: if crack width is larger than 0.2 mm (serviceability limit states: see 5.4), the height of the cracked zone has to be reduced by 10 mm. This rule is only applicable in the ultimate limit state.

  for exposure classes 3 and higher: special provisions have to be taken.

The σ-ε-relation for compressed SFRC is identical to that of plain concrete.

The stresses σ_2 and σ_3 in the σ-ε-diagram are derived from the residual flexural tensile strength as explained below. The residual flexural tensile strengths $f_{R,1}$ and $f_{R,4}$ are calculated considering a linear elastic stress distribution in the section (see 3.5) (Fig. 16a). However, in reality, the stress distribution will be different. To calculate a more realistic stress σ_f in the cracked

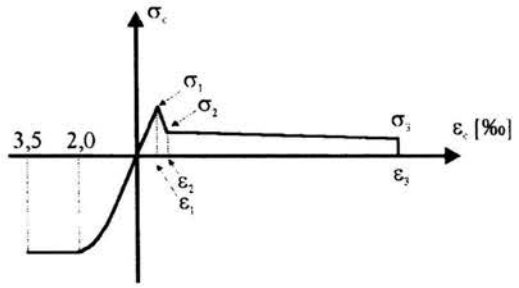

$\sigma_1 = 0.7 f_{\mathrm{fctm,fl}}(1.6 - d)$ (d in m) $[\mathrm{N/mm^2}]$, $\varepsilon_1 = \sigma_1 / E_c$,

$\sigma_2 = 0.45 f_{\mathrm{R},1} \kappa_h$ $[\mathrm{N/mm^2}]$, $\varepsilon_2 = \varepsilon_1 + 0.1‰$,

$\sigma_3 = 0.37 f_{\mathrm{R},4} \kappa_h$ $[\mathrm{N/mm^2}]$, $\varepsilon_3 = 25‰$,

$E_c = 9500 (f_{\mathrm{fcm}})^{1/3}$, $[\mathrm{N/mm^2}]$

χ_h: size factor.

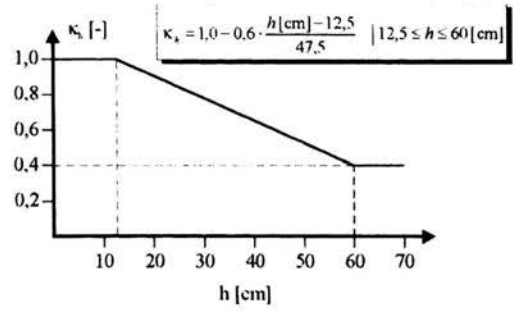

FIGURE 14. Stress-strain diagram and size factor κ_h.

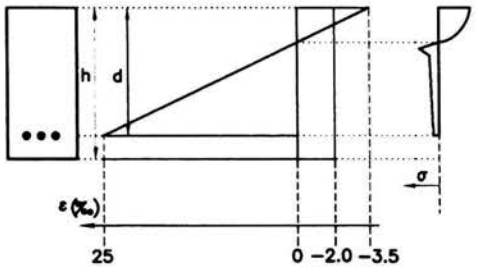

FIGURE 15. Stress and strain distribution.

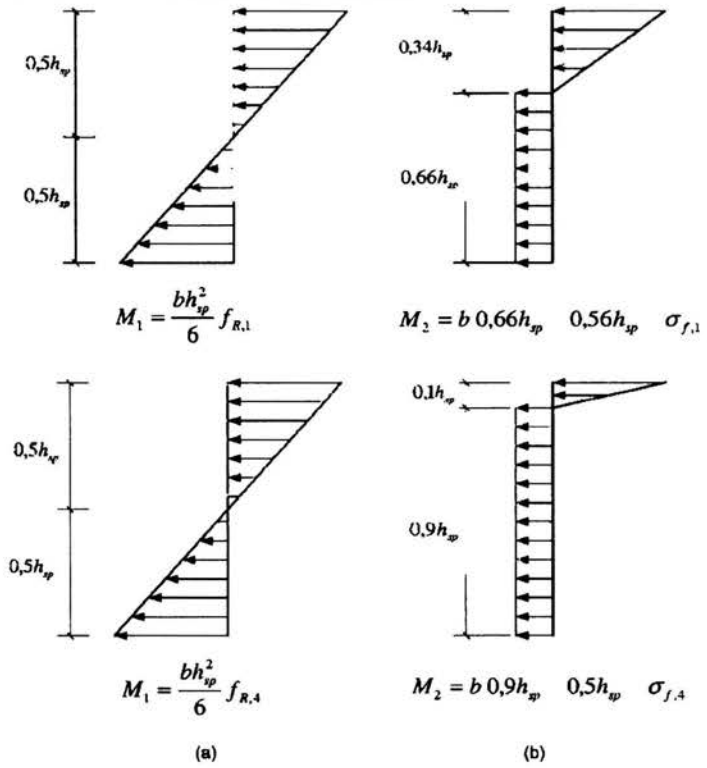

FIGURE 16. Stress distribution.

part of the section, the following assumptions have been made (Fig. 16b):

- the tensile stress Φ_f in the cracked part of the steel fibre concrete section is constant;
- the crack height is equal to $\pm 0.66 h_{\mathrm{sp}}$ at $F_{\mathrm{R},1}$, to $\pm 0.90 h_{\mathrm{sp}}$ at $F_{\mathrm{R},4}$ respectively.

Requiring $M_1 = M_2$, σ_{f} can then be expressed as:

$$\sigma_{\mathrm{f},1} = 0.45 f_{\mathrm{R},1}, \tag{5.8}$$

$$\sigma_{\mathrm{f},4} = 0.37 f_{\mathrm{R},4}. \tag{5.9}$$

5.2.2. Calculation of crack width. Crack control is required in all structures. This crack control can be satisfied by at least one of the following conditions:

- presence of conventional steel bars,
- presence of normal compressive forces (compression – prestressing),

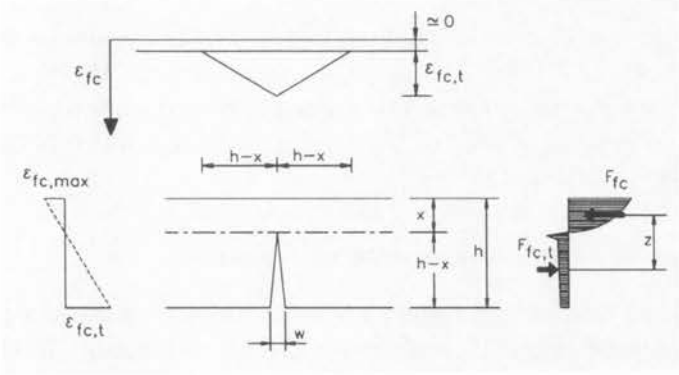

FIGURE 17. Element without ordinary reinforcement.

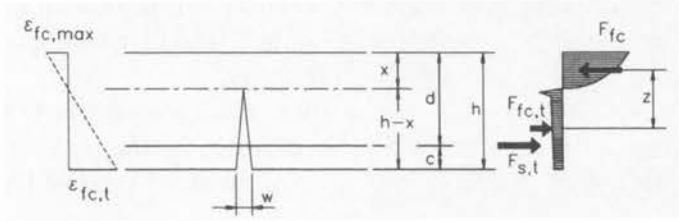

FIGURE 18. Element with ordinary reinforcement.

- crack control maintained by the structural system itself (redistribution of internal moments and forces limited by the rotation capacity).

In structurally indeterminate constructions without conventional reinforcement but with a compression zone in each cross section, the crack width may be determined as follows (see Fig. 17):

- determination of the neutral axis on the basis of Fig. 17,
- determination of the compressive strain $\varepsilon_{fc,max}$ of concrete,
- determination of an idealised tensile strain $\varepsilon_{fc,t}$ taking into account the Bernoulli hypothesis:

$$\varepsilon_{fc,t} = \varepsilon_{fc,max} \frac{h - x}{x}. \tag{5.10}$$

- calculation of the crack width in the ultimate limit state:

$$w = \varepsilon_{fc,t} (h - x). \tag{5.11}$$

In statically determinate constructions (bending - pure tension), crack control is only possible if a high amount of steel fibres is used or if there is a combination of steel fibres and conventional reinforcement.

In structures with conventional reinforcement the calculation of the crack width corresponds to that of normal reinforced concrete. However, the stress in the steel bars has to be calculated, taking into account the beneficial effect of the steel fibres, i.e. a part of the tensile force $F_{fc,t}$ which is taken up by the steel fibres (see Fig. 18).

5.3. Design at ultimate limit states: shear

The calculation for shear shown here applies to beams and plates containing traditional flexural reinforcement (bar and mesh). It also applies to prestressed elements and columns in which axial compression forces are present. The approach proposed is the best possible until further evidence becomes available. When no longitudinal reinforcement or compression zone is available, no generally accepted calculation method for taking into account the effect of the steel fibres can be formulated.

Bent-up bars shall not be used as shear reinforcement in beams except in combination with steel fibres and/or stirrups. In this case at least 50% of the necessary shear reinforcement shall be provided by steel fibres and/or stirrups.

For shear design of members with constant depth, the member is assumed to consist of compressive and tensile zones of which the centres are separated by a distance equal to the internal lever arm z (Fig. 19). The shear zone has a depth equal to z and width b_w. The internal lever arm is calculated perpendicular to the longitudinal reinforcement by ignoring the effect of any bent-up longitudinal reinforcement.

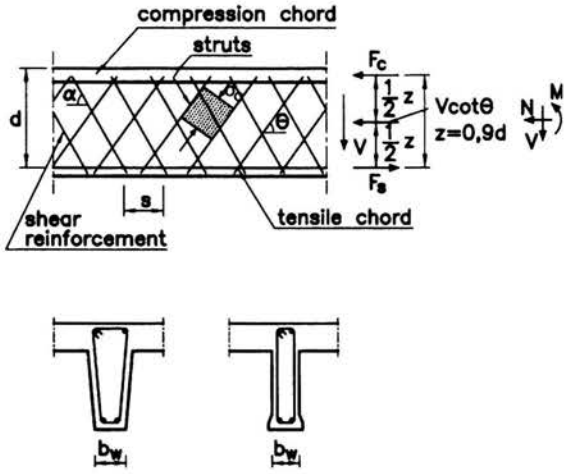

FIGURE 19. Strut and tie model.

The parameters given in Fig. 19 are:

α: the angle of the shear reinforcement in relation to the longitudinal axis ($45° \leq \alpha \leq 90°$),

θ: the angle of the concrete struts in relation to the longitudinal axis,

F_s: tensile force in the longitudinal reinforcement [N],

F_c: compressive force in the concrete in the direction of the longitudinal axis [N],

b_w: minimum width of the web [mm],

d: effective depth [mm],

s: spacing of stirrups [mm],

z: the internal lever arm corresponding to the maximum bending moment in the element under consideration [mm] in a member with constant depth. In the shear analysis, an approximate value $z = 0.9d$ can normally be used.

The standard method, i.e.: $\theta = 45°$, will be used for the shear analysis.

5.3.1. Standard method. The design shear resistance of a section of a beam with shear reinforcement and containing steel fibres is given by the equation:

$$V_{Rd,3} = V_{cd} + V_{fd} + V_{wd}, \tag{5.12}$$

with: V_{cd}: the shear resistance of the member without shear reinforcement given by [18]:

$$V_{cd} = \left\{0.12k\,(100\rho_l f_{ck})^{1/3} + 0.15\sigma_{cp}\right\} b_w d, \qquad \text{[N]} \tag{5.13}$$

where

$$k = 1 + \sqrt{\frac{200}{d}} \qquad \text{(d in mm) and } k \leq 2, \tag{5.14}$$

$$\rho_l = \frac{A_s}{b_w d} \leq 2\%. \tag{5.15}$$

Here: A_s = area of tension reinforcement extending not less than "d+ anchorage length" beyond the section considered (Fig. 20) (mm^2); b_w = minimum width of the section over the effective depth d [mm].

$$\sigma_{cp} = \frac{N_{Sd}}{A_c} \quad (N/mm^2), \tag{5.16}$$

N_{Sd} = longitudinal force in section due to loading or prestressing (compression: positive) [N]. In the case of prestressing, "h" should be used in stead of

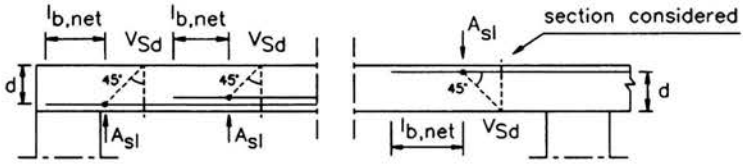

FIGURE 20. ρ_1 for V_{cd}.

"d" in formula (5.13). V_{fd}: contribution of the steel fibre shear reinforcement given by:

$$V_{fd} = 0.7 k_f k_1 \tau_{fd} b_w d \qquad [\mathrm{N}], \tag{5.17}$$

where k_f = factor for taking into account the contribution of the flanges in a T-section:

$$k_f = 1 + n\left(\frac{h_f}{b_w}\right)\left(\frac{h_f}{d}\right) \quad \text{and} \quad k_f \leq 1.5, \tag{5.18}$$

with h_f = height of the flanges [mm], b_f = width of the flanges [mm], b_w = width of the web [mm]

$$n = \frac{b_f - b_w}{h_f} \leq 3 \quad \text{and} \quad n \leq \frac{3b_w}{h_f},$$

$$k_1 = 1 + \sqrt{\frac{200}{d}} \quad (d \text{ in mm}) \quad \text{and} \quad k \leq 2, \tag{5.19}$$

τ_{fd} = design value of the increase in shear strength due to steel fibres:

$$\tau_{fd} = 0.12 f_{Rk,4} \qquad [\mathrm{N/mm^2}], \tag{5.20}$$

V_{wd}: contribution of the shear reinforcement due to stirrups and/or inclined bars, given by:

$$V_{wd} = \frac{A_{sw}}{s} 0.9 d f_{ywd} (1 + \cot\alpha) \sin\alpha \qquad [\mathrm{N}], \tag{5.21}$$

where s = spacing between the shear reinforcement measured along the longitudinal axis [mm], α = angle of the shear reinforcement with the longitudinal axis, f_{ywd} = design yield strength of the shear reinforcement ($\mathrm{N/mm^2}$).

When checking against crushing at the compression struts, V_{Rd2} is given by the equation:

$$V_{Rd,2} = \frac{1}{2} \nu f_{cd} 0.9 d b_w (1 + \cot\alpha) \qquad [\mathrm{N}], \tag{5.22}$$

with

$$\nu = 0.7 - \frac{f_{\mathrm{fck}}}{200} \geq 0.5 \quad (f_{\mathrm{fck}} \text{ in } \mathrm{N/mm^2}). \tag{5.23}$$

For vertical stirrups, or for vertical stirrups combined with inclined shear reinforcement, $\cot\alpha$ is taken as zero.

5.4. Design at serviceability limit states

5.4.1. General. When an uncracked section is used, the full steel fibre reinforced concrete section is assumed to be active and both concrete and steel are assumed to be elastic in tension as well as in compression.

When a cracked section is used, the steel fibre reinforced concrete is assumed to be elastic in compression, and capable of sustaining a tensile stress equal to $0.45 f_{\mathrm{R},1}$.

5.4.2. Limit states of cracking. In the absence of specific requirements (e.g. watertightness), the criteria for the maximum design crack width (w_d) under the quasi-permanent combination [12] of loads, which are mentioned in Table 4 for different exposure classes [12], may be assumed.

TABLE 4. Criteria for crack width.

Exposure class[12]	steel fibres	steel fibres + ordinary reinforcement	steel fibres +	
			post-tensioning	pre-tensioning
1	(**)	(**)	0.2 mm	0.2 mm
2	0.3 mm	0.3 mm	0.2 mm	decompression (*)
3	special crack limitations dependent upon the nature of the aggressive environment involved have to be taken			
4				
5				

(*): the decompression limit requires that, under the frequent combination of loads [12], all parts of the tendons or ducts lie at least 25 mm within concrete in compression

(**): for exposure class 1 [12], crack width has no influence on durability and the limit could be relaxed or deleted unless there are other reasons for its inclusion.

5.4.3. Minimum reinforcement. The following formula is proposed for calculating the minimum reinforcement A_{s} in order to obtain controlled crack formation:

$$A_{\mathrm{s}} = (k_{\mathrm{c}} k k_{\mathrm{p}} f_{\mathrm{fct,ef}} - 0.45 f_{\mathrm{Rm},1}) \frac{A_{\mathrm{ct}}}{\sigma_{\mathrm{s}}} \quad (\mathrm{mm^2}), \tag{5.24}$$

where:

$f_{Rm,1}$ = the average residual flexural tensile strength of the steel fibre reinforced concrete at the moment when a crack is expected to occur (N/mm^2).

A_s = area of reinforcement within tensile zone (mm^2). If A_s is smaller than zero only steel fibres are necessary.

A_{ct} = area of concrete within tensile zone (mm^2). The tensile zone is that part of the section which is calculated to be in tension just before formation of the first crack.

σ_s = the maximum stress permitted in the reinforcement immediately after formation of the crack (N/mm^2). This may be taken equal to the yield strength of the reinforcement (f_{yk}). However, a lower value may be needed to satisfy the crack width limits.

$f_{fct,ef}$ = the tensile strength of the concrete effective at the time when the cracks may first be expected to occur (N/mm^2). In some cases, depending on the ambient conditions, this may be within 3 – 5 days from casting. Values of $f_{fct,ef}$ may be obtained from formula (5.1) by taking as f_{fck} the strength at the time cracking is expected to occur. When the time of cracking cannot be established with confidence as being less than 28 days, it is recommended that a minimum tensile strength of $3\,N/mm^2$ be adopted.

k_c = a coefficient which takes account of the nature of the stress distribution within the section immediately prior to cracking. The relevant stress distribution is that resulting from the combination of effects of loading and restrained imposed deformations.
$k_c = 1$ for pure tension ($e = M/N = 0$).
$k_c = 0.4$ for bending without normal compressive force ($e = \infty$).
In the range between $e = 0$ and $e = \infty$:

- $e/h < 0.4$

$$k_c = \frac{1 + \frac{e}{0.4h}}{1 + \frac{6e}{h}}, \tag{5.25}$$

- $e/h \geq 0.4$

$$k_c = \frac{1 + \frac{0.4h}{e}}{2.5\left(1 + \frac{h}{6e}\right)}, \tag{5.26}$$

k = a coefficient which allows for the effect of non-uniform self-equilibrating stresses. The value can be taken as 0.8 as a first approximation. For further details, see ENV 1992-1-1 [12].

k_p = a coefficient which takes account of the prestressing effect:

$$k_p = 1 - \frac{\alpha}{k_c}\left(1 - k_c + 2.4\frac{e_v}{h} - 6\frac{e_v k_c}{h}\right), \tag{5.27}$$

where:

$$\alpha = \text{ the ratio of prestressing } = \frac{\sigma_{cp}}{k f_{fct,ef}}, \tag{5.28}$$

$$\sigma_{cp} = \frac{N_{Sd}}{A_c} \qquad [\mathrm{N/mm^2}],$$

N_{Sd} = prestressing force [N],

A_c = cross section of concrete ($\mathrm{mm^2}$),

e_v = the eccentricity of the prestressing force [mm].

If $e_v = 0$

$$k_p = 1 - \frac{\alpha}{k_c}(1 - k_c), \tag{5.29}$$

for pure bending ($k_c = 0.4$), it follows that:

$$k_p = 1 - 1.5\alpha. \tag{5.30}$$

5.4.4. Calculation of crack width. Crack control is only possible if at least one of the conditions mentioned in 5.2.2 is satisfied. The calculation of the design crack width in steel fibre reinforced concrete is similar to that in normal reinforced concrete. However, it has to be taken into account that the tensile stress in steel fibre reinforced concrete after cracking is not equal to zero but equal to 0.45 $f_{Rm,1}$ (constant over the cracked part of the cross section).

Equation (5.24) can be used to calculate the reinforcement A_{sr} ($\mathrm{mm^2}$) which satisfies the crack width limit. With $\gamma_R = f_{yk}/\sigma_s = 1.4$ the crack width is approximately limited to 0.25 mm:

$$\frac{A_{sr}}{A_{ct}} = \frac{k_c k_p k f_{fct,ef} - \frac{0.45}{1.4} f_{Rm,1}}{\frac{f_{yk}}{1.4}}. \tag{5.31}$$

In ordinary reinforced concrete, the following formula is used to calculate the crack width:

$$w_k = \beta s_{rm} \varepsilon_{sm}, \tag{5.32}$$

where:

w_k = the design crack width [mm],

s_{rm} = the average final crack spacing [mm],

ε_{sm} = the mean steel strain in the reinforcement allowed under the relevant combination of loads for the effects of tension stiffening, shrinkage, etc.

β = a coefficient relating the average crack width to the design value,

= 1.7 for load induced cracking and for restrained cracking in sections with a minimum dimension in excess of 800 mm,

= 1.3 for restrained cracking in sections with a minimum depth, breadth or thickness (whichever is the lesser) of 300 mm or below.

Values for intermediate section sizes may be interpolated.

ε_{sm} may be calculated from the relation:

$$\varepsilon_{sm} = \frac{\sigma_s}{E_s}\left[1 - \beta_1\beta_2\left(\frac{\sigma_{sr}}{\sigma_s}\right)^2\right], \tag{5.33}$$

where:

σ_s = the stress in the tensile reinforcement calculated on the basis of a cracked section (N/mm^2),

σ_{sr}= the stress in the tensile reinforcement calculated on the basis of a cracked section under loading conditions causing first cracking (N/mm^2),

β_1 = coefficient which takes account of the bond properties of the bars

= 1.0 for high bond bars,

= 0.5 for plain bars,

β_2 = a coefficient which takes account of the duration of the loading or of repeated loading,

= 1.0 a for single, short term loading,

= 0.5 for a sustained load or for many cycles of repeated loading.

For members subjected only to intrinsic imposed deformations, σ_s may be taken as equal to σ_{sr}.

The average final crack spacing for members subjected principally to flexure or tension can be calculated from the equation [19]:

$$s_{rm} = \left(50 + 0.25k_1k_2\frac{\phi_b}{\rho_r}\right)\left(\frac{50}{L/\phi}\right) \qquad \text{[mm]}, \tag{5.34}$$

where:

$50/(L/\Phi) \leq 1$,

Φ_b = the bar size in mm. Where a mixture of bar sizes is used in a section, an average bar size may be used,

k_1 = a coefficient which takes account of the bond properties of the bars,

k_1 = 0.8 for high bond bars and 1.6 for plain bars. In the case of imposed deformations, k_1 should be replaced by $k_1 \cdot k$, with k being defined in 5.4.3,

k_2 = a coefficient which takes account of the form of the strain distribution. = 0.5 for bending and 1.0 for pure tension,

ρ_r= the effective reinforcement ratio, $A_s/A_{c,eff}$ where A_s is the area of reinforcement contained within the effective tension area $A_{c,eff}$. The effective tension area is generally the area of concrete surrounding the tension reinforcement of depth equal to 2.5 times the distance from the tension face of the section to the centroid of reinforcement [12],

L = length of steel fibre [mm],

Φ = diameter of steel fibre [mm].

For steel fibre reinforced concrete, σ_s and σ_{sr} in (5.33) are calculated taking into account the postcracking tensile strength of the steel fibre reinforced concrete, i.e. $0.45 f_{Rm,1}$, in the cracked part of the section.

5.5. Detailing provisions

The rules applicable to normal reinforcement (bar, mesh) and prestressing tendons can be found in ENV 1992-1-1 [12]. Only requirements applicable to "steel fibre reinforced concrete" will be discussed below.

5.5.1. Shear reinforcement in beams. A minimum shear reinforcement is not necessary for members with steel fibres. But it must be guaranteed that the fibres have a significant influence on the shear resistance. Fibre type and fibre dosage must be sufficient so that a characteristic residual flexural tensile strength $f_{Rk,4}$ of 1 N/mm^2 is achieved.

6. Comments from the BRITE EURAM project: σ-ε-design method [19]

6.1. Limitation with regard to the size factor κ_h

The size factor presented in Fig. 14 is only valid when the stress-strain diagram as shown in Fig. 14 is used. It should be noted for the design processes that the size factor depends on whether multiple or single cracks occur. The larger the crack width in ultimate limit state becomes, the stronger the size effect will be. Furthermore, it should be considered that the size factor is influenced by the fibre length. In the test program presented in [9] only one fibre length (60 mm) was investigated. Theoretical investigations show that for shorter fibres a stronger size effect takes place.

6.2. Serviceability limit state of cracking

The corrosion resistance of cracked concrete ($350\,kg/m^3$ of cement; $W/C = 0.45$) was examined in subtask 5.1 of the Brite Euram project. In all exposure classes, except wetting in 5% NaCl drying in CO_2, no corrosion could be found inside the concrete nor in the cracks up to 0.5 mm during the whole exposure period of 18 months. In some samples wetted in NaCl and dried in CO_2, only superficial brown rust on some fibres bridging the cracks could be found. There was no decrease in fibre diameter.

Out of this research, it may be expected that in the absence of chlorides no corrosion can be expected up to crack widths of 0.5 mm; in the presence of chlorides it is recommended to limit the crack width to 0.2 mm.

The accuracy of the recommended calculation procedure for crack widths in RILEM TC162-TDF has been verified by means of experimental results. The comparison between calculated values and test results shows that especially for larger fibre contents, the agreement is relatively well (see also Section 7).

7. Calculation of crack widths with the σ-ε-design method [1]

It is known that the calculation of crack widths is not an easy job. A lot of complicated parameters, like the postcracking strength and the bond stress-slip relation strongly influence the results. These parameters are not only difficult to determine accurately, but they are also not taken into account or simplified too much by the existing cracking models.

The RILEM TC162-TDF method is a rather easy method that is very close to the approach in Eurocode 2 [12]. However, the method is an empirical method. In search for a more fundamental calculation method, a new physical model has been developed to describe the cracking behaviour of a beam in bending. The model is quite complicated and requires the right input parameters. However, it is not the objective to use this model for daily calculations, but it can help to better understand the mechanism of crack formation.

7.1. Development of a new physical model to simulate the formation and growth of cracks

7.1.1. Calculation of crack spacing. When a beam is loaded with a bending moment or axial tensile force, the tensile force is carried partially by the reinforcement bars and partially by the concrete. If the load is increased and the concrete tensile stress reaches the tensile strength, cracks are formed

in the weakest sections. For plain concrete, all of the tensile force is taken by the reinforcement bar at the place of the crack. For SFRC the fibres also carry a part of the tensile force, but this part is still smaller than the part carried by the concrete before cracking. Else the material would be strain hardening. The difference in tensile force carried by the reinforcement bars before cracking and after cracking is gradually transferred to the concrete by bond stresses. The anchorage length is defined here as the distance needed to transfer this difference in tensile force. In other words, the anchorage length is the distance between a crack and the nearest section where the strain in the reinforcement bar is equal to the strain in the surrounding concrete. Over this distance the tensile stress in the concrete is reduced. Therefore, at the moment of cracking it is impossible that two cracks are formed with a crack spacing smaller than 2 times the anchorage length. It is assumed that all the first-order cracks are formed when the bending moment reaches a value of 1.2 times the cracking moment. When the load is further increased second order cracks are formed in between the first order cracks. After the completion of the second-order cracking pattern, the minimum distance between two cracks is equal to the anchorage length. The maximum distance is equal to 2 times the anchorage length. From this it is concluded that the average crack spacing is equal to 1.5 times the anchorage length.

In Fig. 21, a fragment of a beam is shown. The beam is loaded with a constant bending moment M_{cr} equal to the cracking moment if the tensile strength would be $1.2f_{ct}$. The tensile strength f_{ct} is the flexural tensile strength, corrected for the depth of the beam and determined according to Fig. 14. Section 2 is a cracked section, while section 1 is a section that is just about to crack. The general calculation procedure consists of two steps. In a first step the anchorage length L in Fig. 21 is determined, assuming that the tensile stress in section 1 is equal to 1.2 times the tensile strength f_{ct} and furthermore assuming that the cracking stress in section 1 is equal to 0.8 times the tensile strength f_{ct}. These last assumptions are made to take into account the scatter observed in the experimental determination of the tensile strength.

It is furthermore assumed that the influence of the fibres in section 2 can be simulated with a drop-constant stress-strain relation. The stress σ_f is calculated as $0.39 \cdot f_{R,1}$ (see paragraph 5.7 in [1] and Fig. 21). Section 1 is an uncracked section where the strain in the reinforcement bars is equal to the strain in the surrounding concrete. The position of the neutral axis can be calculated exactly in sections 1 and 2 by means of a static equilibrium of axial forces and bending moments. For sections that lie in between section 1 and 2 it is assumed that the position of the neutral axis is constant over

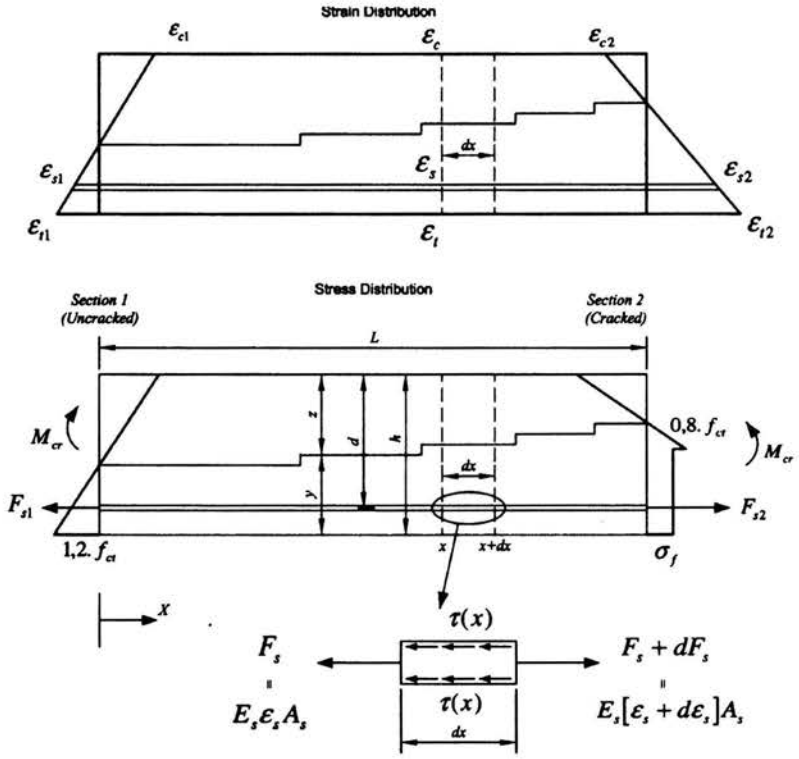

FIGURE 21. Beam part between a cracked section and a section that has just reached the point of cracking.

a small interval and can be calculated as follows:

$$z_x = z_1 + \frac{z_2 - z_1}{\delta_2}\delta_x, \tag{7.1}$$

where:

z_x = the position of the neutral axis at place x [mm];

z_1 and z_2 are the positions of the neutral axis in section 1 and 2, respectively [mm];

δ_2 = the slip between reinforcement and surrounding concrete in section 2 [mm];

δ_x = the slip between reinforcement and surrounding concrete in place x [mm].

Equation (7.1) is an assumption, based on the observation that the position of the neutral axis varies in the same way over the length L as the slip δ. To start the calculations a value of δ_2 must be assumed and afterwards, if

this slip was not correct, an iteration step can be performed. Convergence is very fast.

In step one the unknown parameters are:

- the length L [mm];
- the steel strain in section 1: ε_{s1};
- the steel strain in section 2: ε_{s2};
- the compressive strain in section 1: ε_{c1};
- the compressive strain in section 2: ε_{c2};
- the position of the neutral axis: y and z [mm];
- the slip δ as function of x [mm].

For the calculation of the length L and slip δ, a differential equation must be solved. All other unknown parameters can be solved by simple static equilibrium of forces and moments. According to the hypothesis of Bernoulli the following relations can be written:

$$\varepsilon_{s1} = \varepsilon_{t1}\frac{d - z_1}{y_1}, \qquad \varepsilon_{s2} = \varepsilon_{t2}\frac{d - z_2}{y_2}, \tag{7.2}$$

$$\varepsilon_{c1} = \varepsilon_{t1}\frac{z_1}{y_1}, \qquad \varepsilon_{c2} = \varepsilon_{t2}\frac{z_2}{y_2}. \tag{7.3}$$

The hypothesis of Bernoulli is only valid in sections 1 and 2. In all other sections, the strain in the reinforcement bar is different from the strain in the surrounding concrete. In reality this is also the case in section 2, where the real tensile strain in the concrete is equal to the postcracking tensile strength divided by Young's modulus. However, by adding to this real tensile strain the contribution of the crack width (w/L_{ch}) (L_{ch} = characteristic length), a virtual strain is obtained in section 2. This virtual stress-strain relation in section 2 makes that it is reasonable to assume that the strain in the reinforcement is equal to the strain in the surrounding concrete in section 2. Requiring static equilibrium of normal forces for section 1 results in:

$$\frac{1}{2}bz_1E_c\varepsilon_{c1} = \frac{1}{2}by_1E_c\varepsilon_{t1} + A_sE_s\varepsilon_{s1} - A_sE_c\varepsilon_{t1}\frac{d - z_1}{y_1}, \tag{7.4}$$

with:

E_c: Young's modulus of concrete (N/mm^2),

E_s: Young's modulus of steel (N/mm^2),

A_s: steel section (mm^2),

d: effective depth of the beam [mm],

b: width of the beam [mm].

Requiring static equilibrium of normal forces in section 2 results in:

$$\frac{1}{2}bz_2E_c\varepsilon_{c2} = \frac{1}{2}by_2 0.8f_{ct}\frac{0.8\varepsilon_{ct}}{\varepsilon_{t2}} + by_2\sigma_f\left(1 - \frac{0.8\varepsilon_{ct}}{\varepsilon_{t2}}\right) + A_sE_s\varepsilon_{s2} - A_s\sigma_f. \quad (7.5)$$

Requiring static equilibrium of moments for section 1 results in:

$$\frac{1}{3}bz_1^2E_c\varepsilon_{c1} + \frac{1}{3}by_1^2E_c\varepsilon_{t1} + A_sE_s\varepsilon_{s1}(d - z_1) - A_sE_c\varepsilon_{t1}\frac{(d - z_1)^2}{y_1} = M. \quad (7.6)$$

Requiring static equilibrium of moments for section 2 results in:

$$\frac{1}{3}bz_2^2E_c\varepsilon_{c2} + \frac{1}{3}by_2^2 0.8f_{ct}\left(\frac{0.8\varepsilon_{ct}}{\varepsilon_{t2}}\right)^2 + \left(by_2^2\sigma_f\left(1 - \frac{0.8\varepsilon_{ct}}{\varepsilon_{t2}}\right)\right)\left(\frac{0.8\varepsilon_{ct}}{2\varepsilon_{t2}} + \frac{1}{2}\right) + (A_sE_s\varepsilon_{s2} - A_s\sigma_f)(d - z_2) = M. \quad (7.7)$$

From equations (7.4) to (7.7) the strain distributions in sections 1 and 2 can be calculated. This results in the complete knowledge of stresses and strains in sections 1 and 2. The only remaining unknown parameters are the length L and the slip δ as a function of x. If a static equilibrium of normal forces and moments is written for an arbitrary section at place x, the following equations are found:

$$\frac{1}{2}bzE_c\varepsilon_c = \frac{1}{2}byE_c\varepsilon_t + A_s\left(E_s\varepsilon_s - E_c\varepsilon_t\frac{d - z}{y}\right), \quad (7.8)$$

$$\frac{1}{3}bz^2E_c\varepsilon_c + A_s\left(E_s\varepsilon_s - E_c\varepsilon_t\frac{d - z}{y}\right)(d - z) + \frac{1}{3}by^2E_c\varepsilon_t = M. \quad (7.9)$$

Extracting ε_c from equation (7.8) gives:

$$\varepsilon_c = \frac{y}{z}\varepsilon_t + \frac{2A_s}{bzE_c}\left(E_s\varepsilon_s - E_c\varepsilon_t\frac{d - z}{y}\right). \quad (7.10)$$

Substituting equation (7.10) into equation (7.9) gives:

$$\frac{1}{3}bz^2E_c\left[\frac{y}{z}\varepsilon_t + \frac{2A_s}{bzE_c}\left(E_s\varepsilon_s - E_c\varepsilon_t\frac{d - z}{y}\right)\right] + A_s\left(E_s\varepsilon_s - E_c\varepsilon_t\frac{d - z}{y}\right)(d - z) + \frac{1}{3}by^2E_c\varepsilon_t = M. \quad (7.11)$$

From equation (7.11), ε_t can be written as a function of ε_s:

$$\varepsilon_t = \frac{M - A_sE_s\varepsilon_s\left(d - \frac{z}{3}\right)}{\frac{1}{3}byhE_c - A_sE_c\frac{d-z}{y}\left(d - \frac{z}{3}\right)}. \quad (7.12)$$

This leaves only the strain ε_s to be determined. Since the steel rebars are slipping relative to the surrounding concrete, the steel strain is composed of two parts. The first part is the strain of the surrounding concrete, while the second part is the strain due to the slipping of the rebars:

$$\varepsilon_s = \varepsilon_t \frac{d-z}{y} + \frac{d\delta(x)}{dx}. \tag{7.13}$$

Equation (7.12) is substituted in equation (7.13):

$$\frac{d\delta(x)}{dx} = \varepsilon_s - \frac{M - A_s E_s \varepsilon_s \left(d - \frac{z}{3}\right)}{\frac{1}{3} b y h E_c - A_s E_c \frac{d-z}{y} \left(d - \frac{z}{3}\right)} \cdot \frac{d-z}{y}. \tag{7.14}$$

If the derivative of equation (7.14) is calculated, then equation (7.15) is found. It is assumed here that the moment M is independent on the position x along the longitudinal axis, i.e. the bending moment is constant in this zone of the beam. Furthermore the position of the neutral axis (z and y) is assumed to be constant over a small interval. In each small interval the value of z and y can be calculated by means of equation (7.1):

$$\frac{d^2\delta(x)}{dx^2} = \frac{d\varepsilon_s}{dx} \left[1 + \frac{A_s E_s \left(d - \frac{z}{3}\right)(d-z)}{\frac{1}{3} b y^2 h E_c - A_s E_c (d-z)\left(d - \frac{z}{3}\right)} \right]. \tag{7.15}$$

To solve this differential equation a relation must be found between the slip δ and the strain ε_s, both functions of x. The horizontal equilibrium of the steel reinforcement between the place x and the place $x + dx$ results in (Fig. 21):

$$\underbrace{A_s E_s \varepsilon_s + \tau(x) \cdot \pi \cdot \sigma\phi \cdot dx = A_s E_s (\varepsilon_s + d\varepsilon_s)}_{\frac{d\varepsilon_s}{dx} = \tau(x) \frac{\pi \cdot \sigma\phi}{E_s A_s}}. \tag{7.16}$$

Substituting expression (7.16) in equation (7.15) results in:

$$\frac{d^2\delta(x)}{dx^2} = \tau(x) \underbrace{\frac{\pi \cdot \sigma\phi}{E_s A_s} \left[1 + \frac{A_s E_s \left(d - \frac{z}{3}\right)(d-z)}{\frac{1}{3} b y^2 h E_c - A_s E_c (d-z)\left(d - \frac{z}{3}\right)} \right]}_{A}. \tag{7.17}$$

Now only a relation has to be assumed describing τ as a function of $\delta(x)$. This chosen τ-δ-relation is equation (7.18).

$$\tau = \tau_{max} \left(1 - \mu e^{-\lambda\delta}\right). \tag{7.18}$$

The determination of $\tau_{\max}$ is explained in [20-22]. The parameters μ and λ can be determined as explained in paragraph 7.2.4 of [1]. Substituting equation (7.18) in equation (7.17) gives:

$$\frac{d^2\delta(x)}{dx^2} = A\,\tau_{\max}\left(1 - \mu e^{-\lambda\delta(x)}\right). \tag{7.19}$$

The solution of equation (7.19) is analogue as the procedure explained by Vandewalle [12] for tension bars in plain concrete. A few new parameters are introduced:

$$\lambda \cdot \delta(x) = \varphi(x) \quad \underbrace{\sqrt{\tau_{\max} \cdot A \cdot \lambda}}_{a} \cdot x = \alpha \quad p = \frac{d\varphi}{d\alpha} = \varphi'. \tag{7.20}$$

Equation (7.19) can now be written as:

$$\underbrace{\varphi'' = \frac{dp}{d\alpha} = \frac{dp}{d\varphi}\frac{d\varphi}{d\alpha} = \frac{dp}{d\varphi}p = \varphi'\frac{d\varphi'}{d\varphi}}_{\Downarrow} \tag{7.21}$$

$$\varphi'\frac{d\varphi'}{d\varphi} = 1 - \mu e^{-\varphi}$$

$$\Downarrow$$

$$\varphi' d\varphi = \left(1 - \mu e^{-\varphi}\right) d\varphi.$$

If this last expression is integrated, equation (7.22) is obtained:

$$\varphi'^2 = 2\int \left(1 - \mu\, e^{-\varphi}\right) d\varphi \tag{7.22}$$

$$\Downarrow$$

$$\varphi'^2 = 2\left[\varphi + \mu \cdot e^{-\varphi}\right] + C_1.$$

For the determination of the integration constant C_1 the following boundary conditions have been taken into account:

$$\text{For } x = 0 \rightarrow \begin{cases} \delta = 0 \Rightarrow \varphi = 0, \\ \frac{d\delta}{dx} = 0 \Rightarrow \varphi' = 0. \end{cases} \tag{7.23}$$

This results in:

$$C_1 = -2\mu. \tag{7.24}$$

Equation (7.22) can now be used to determine the course of the slip δ as function of x:

$$\varphi' = \frac{d\varphi}{d\alpha} = \sqrt{2\,(\varphi + \mu\,\mathrm{e}^{-\varphi}) - 2\mu} \tag{7.25}$$

$$\Downarrow$$

$$\int_0^{\alpha} d\alpha = \int_0^{\varphi} \frac{d\varphi}{\sqrt{2\,(\varphi + \mu \mathrm{e}^{-\varphi}) - 2\mu}}.$$

Integrating expression (7.25) leads to:

$$\alpha + C_2 = ax + C_2 = \int \underbrace{\frac{d\varphi}{\sqrt{2\,(\varphi + \mu \mathrm{e}^{-\varphi}) - 2\mu}}}_{F}. \tag{7.26}$$

The integration constant C_2 in equation (7.26) is determined with the following boundary condition:

$$x = 0 \rightarrow \begin{cases} \alpha = 0, \\ \delta = 0 \Rightarrow \varphi = 0. \end{cases} \tag{7.27}$$

Equation (7.26) cannot be solved analytically. If x and δ are equal to 0, the function F is infinite. Therefore, a numerical procedure has been worked out in which the exponential function contained in the function F is replaced by [20]:

$$\mathrm{e}^{-\varphi} = 1 - 0.9664\varphi + 0.3536\varphi^2. \tag{7.28}$$

Equation (7.26) can now be written as:

$$\alpha + C_2 = ax + C_2 = \int \underbrace{\frac{d\varphi}{\sqrt{2\varphi - 1.9328\varphi + 0.7072\varphi^2}}}_{F}. \tag{7.29}$$

Assume that:

$$\left.\begin{aligned} t &= 1 + c\varphi \\ c &= \frac{0.7072\mu}{1 - 0.9664\mu} \end{aligned}\right\} \Rightarrow \begin{aligned} t^2 - 1 &= 2c\varphi + c^2\varphi^2, \\ dt &= cd\varphi. \end{aligned} \tag{7.30}$$

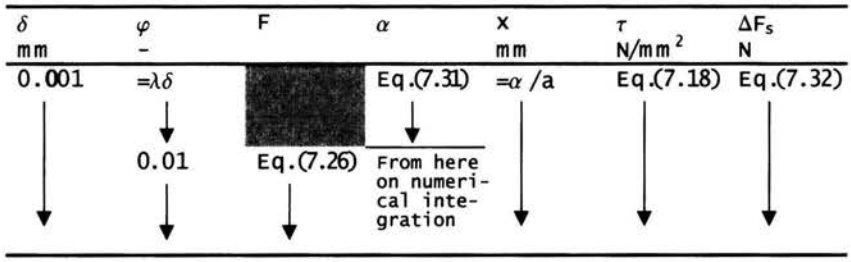

FIGURE 22. Calculation scheme for the determination of the anchorage length.

Then it follows that:

$$\underbrace{\alpha + C_2 = ax + C_2 = \frac{1}{\sqrt{c(1 - 0.9664\mu)}} \int \frac{dt}{\sqrt{t^2 - 1}}}_{\Downarrow} \tag{7.31}$$

$$\alpha + C_2 = \frac{1}{\sqrt{c(1 - 0.9664\mu)}} \ln \left| t + \sqrt{t^2 - 1} \right|.$$

If x and δ are 0, then α is also 0 and t is equal to 1. Hence it follows from equation (7.31) that C_2 is equal to 0. The function (7.31) is only used for values of φ that are in the very close neighbourhood of 0. If φ becomes larger than 0.01, the function F is further used to make a numerical integration. Practically, the length L can now be determined with a simple excel sheet (Fig. 22).

For a series of δ values the corresponding value of x is calculated with equation (7.31) or by means of numerical integration of equation (7.26). With each value of δ, also a value of τ can be associated. Once τ is known as a function of x, the total shear force ΔF_s can be numerically calculated. The anchorage length is found as the value of x for which the total shear force is equal to the difference in steel force between section 1 and section 2:

$$\Delta F_s = A_s E_s (\varepsilon_{s2} - \varepsilon_{s1}) = \pi \cdot \sigma\phi \cdot \int_0^L \tau(x) dx. \tag{7.32}$$

Following the above explained approach the length L can be determined. The average final crack spacing is now assumed equal to $1.5L$.

7.1.2. Calculation of the crack width. In the second step of the calculation, the crack widths are calculated for a series of bending moments.

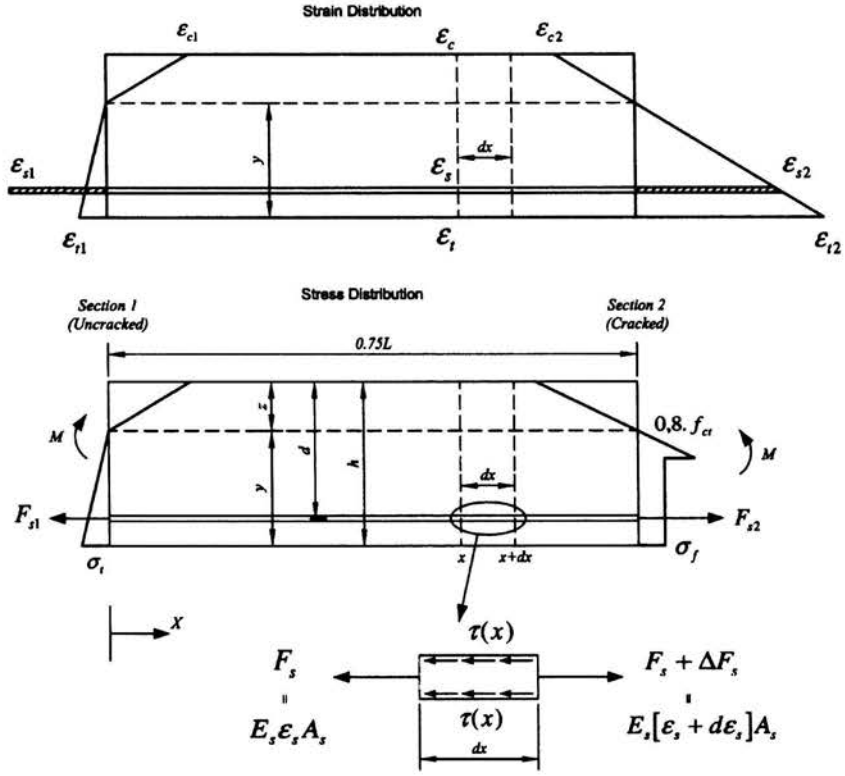

FIGURE 23. Beam fragment between a cracked section and a section that is situated in the middle of two cracks.

Therefore, the length of the model is now fixed at half the average final crack spacing or $0.75L$. In section 2, the boundary conditions remain the same, but in section 1, the strain distribution is now different. Since the length of the model is no longer L, the stress in the bottom fibre of section 1 is now lower than the tensile strength.

Also in section 1 the strain in the reinforcement is no longer equal to the strain in the surrounding concrete. The neutral axis in section 1 will be higher than in the first step of the calculation. Furthermore, due to the close presence of the crack, the assumption of Bernoulli (plane sections remain plane) is no longer valid in section 1. This results in 4 unknown parameters for section 1: the steel strain ε_{s1}, the tensile strain in the concrete ε_{t1}, the compressive strain in the concrete ε_{c1} and the position of the neutral axis z_1. To be able to solve the problem, one of the unknown parameters must be chosen. In this case it is assumed that the neutral axis is at the same position as in section 2. Later on the calculations will show that the position of the neutral axis in section 1 has virtually no influence on the calculation of the

crack width. This leaves only the 3 strains in section 1 to be determined. By means of a static equilibrium of axial forces and bending moments, the strains ε_{c1} and ε_{t1} can be written as a function of ε_{s1} (see equations (7.10) and (7.12)). ε_{s1} is found by iteration. First a value of ε_{s1} is assumed. With this value, equation (7.22) is solved. Due to the fact that the strain in the reinforcement is no longer equal to the strain in the surrounding concrete, the boundary conditions in section 1 are now changed:

$$\text{For } x = 0 \rightarrow \begin{cases} \delta = 0 \Rightarrow \varphi = 0, \\ \frac{d\delta}{dx} = \varepsilon_{s1} - \varepsilon_{t1}\frac{d-z_1}{y_1} \Rightarrow \varphi' = \frac{\lambda\cdot\varepsilon_{s1}}{a} - \frac{\lambda}{a}\varepsilon_{t1}\frac{d-z_1}{y_1}. \end{cases} \tag{7.33}$$

This results in a new integration constant:

$$C_1 = \left[\frac{\lambda\varepsilon_{s1}}{a} - \frac{\lambda\varepsilon_{t1}}{a}\left(\frac{d-z_1}{y_1}\right)\right]^2 - 2\mu. \tag{7.34}$$

From equation (7.22) and (7.34) the following relation can be derived:

$$\left[\frac{\lambda\varepsilon_s}{a} - \frac{\lambda\varepsilon_t\,(d-z)}{ay}\right]^2 = 2\left[\varphi + \mu e^{-\varphi}\right] + \left[\frac{\lambda\varepsilon_{s1}}{a} - \frac{\lambda\varepsilon_{t1}\,(d-z)}{ay}\right]^2 - 2\mu. \tag{7.35}$$

If the relation found in equation (7.12) is filled into equation (7.35), an expression is found for the strain ε_s as function of x:

$$\varepsilon_s = \frac{\sqrt{2\left[\varphi + \mu e^{-\varphi}\right] + \left[\frac{\lambda\varepsilon_{s1}}{a} - \frac{\lambda\varepsilon_{t1}(d-z)}{ay}\right]^2 - 2\mu}\cdot\left[\frac{bhyE_c}{3} - A_sE_c\left(\frac{d-z}{y}\right)\left(d-\frac{z}{3}\right)\right]}{\frac{\lambda}{a}\left[\frac{bhyE_c}{3} + A_s\left(E_s - E_c\right)\left(\frac{d-z}{y}\right)\left(d-\frac{z}{3}\right)\right]}$$

$$+ \frac{(d-z)\cdot M}{y\left[\frac{bhyE_c}{3} - A_sE_c\left(\frac{d-z}{y}\right)\left(d-\frac{z}{3}\right)\right] + (d-z)\,A_sE_s\left(d-\frac{z}{3}\right)}. \tag{7.36}$$

For the chosen value of ε_{s1} the value of ε_s is calculated by means of equation (7.36) for x equal to $0.75L$. This is done in the following way: Using equation (7.36) a new column can be added to in Fig. 22 in which the strain ε_s is calculated. In the table the value of ε_s can be found that corresponds to $x = 0.75L$. This strain ε_s must be equal to the strain ε_{s2} that was determined from equations (7.5) and (7.7). The procedure is repeated, each time for a new ε_{s1}, until the demand is satisfied. Once this has been done the average crack width is found as twice the value of the slip δ at a distance $x = 0.75L$.

7.2. Experimental program

At the Department of Civil Engineering of the Catholic University of Leuven(Belgium) a test program was executed that involved 4-point bending tests on 19 full-scale beams. All beams had a depth of 300 mm and a width of 200 mm. The span was always equal to 2300 mm. The investigated parameters for the 19 beams were the reinforcement ratio, the fibre dosage and the fibre type. The concrete cover on the longitudinal reinforcement is equal to 30 mm. Details for all beams can be found in Table 5.

TABLE 5. Test parameters.

Beam	Fibre dosage kg/m^3	Fibre type	Span (*) mm	Reinforcement # ϕx [mm]
1	0	-	1000	3 ϕ20
2	20	RC 65/60 BN (**)	1000	3 ϕ20
3	60	RC 65/60 BN	1000	3 ϕ20
4	0	-	1000	3 ϕ16
5	20	RC 65/60 BN	1000	3 ϕ16
6	60	RC 65/60 BN	1000	3 ϕ16
7	0	-	1000	3 ϕ16
8	20	RL 45/50 BN	1000	3 ϕ16
9	60	RL 45/50 BN	1000	3 ϕ16
10	0	-	1000	3 ϕ20
11	20	RL 45/50 BN	1000	3 ϕ20
12	60	RL 45/50 BN	1000	3 ϕ20
13	40	RC 65/60 BN	1000	3 ϕ16
14	40	RC 80/35 BN	1000	3 ϕ16
15	60	RC 80/35 BN	1000	3 ϕ16
16	40	RC 65/60 BN	1000	3 ϕ20
17	0	-	1500	3 ϕ20
18	20	RC 65/60 BN	1500	3 ϕ20
19	60	RC 65/60 BN	1500	3 ϕ20

(*): Span means here the zone between the loading points (= zone of constant moment in which the crack widths are measured)

(**): R: hooked end fibre - C: fibres are glued in bundles, L: fibres are not glued - 65: aspect ratio of fibre (=length/diameter = L/ϕ) - 60: length of fibre (= L in mm) - B: no coating - N: low carbon, i.e. minimum yield strength of 1100 MPa.

A picture of the test set-up is shown in Fig. 24. All beams were tested under load control. The size of the load steps was so that the beam failed after 10 to 15 load steps. After each load step, the deflection was measured as well as the crack widths on both sides of the beam. The crack widths were measured at $\pm$ 1 cm above the bottom of the beam, only in the zone of constant moment (between the loading points). The measurement of the crack widths was done with a small, calibrated microscope. The smallest scale

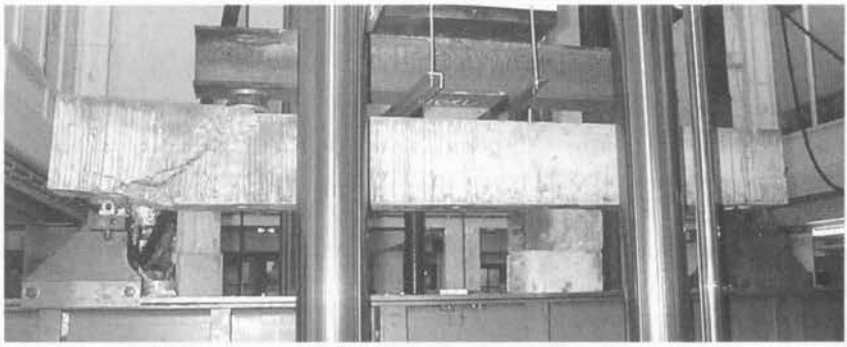

FIGURE 24. Test set-up for all beams.

division in the microscope corresponds to 0.02 mm. Furthermore, due to the freaky shapes of the cracks it was sometimes difficult to decide how large the crack width was. Finally, it must be said that a crack width can only be measured after the crack has been detected. The smallest crack widths that could be detected had already a crack width of 0.02 to 0.03 mm. This implies that the cracks that have a crack width smaller than 0.02 to 0.03 mm are not detected and not taken into account in the calculation of the average crack width. The result is that the average experimentally observed crack width is a little overestimated. The effect of this becomes more important for beams with a high reinforcement ratio and a high fibre dosage, since for these beams the number of very small cracks that remain undetected is higher. For all these reasons, the author thinks that, although the measurements were taken with great care, there is a high degree of uncertainty regarding the test results.

Together with each beam 10 cubes were cast to measure the mean cube compressive strength $f_{cm,cube}$ as well as 8 RILEM 3-point bending specimens to measure the postcracking behaviour. The mean cylinder compressive strength f_{cm} is taken equal to $0.8 \cdot f_{cm,cube}$. The Young's modulus of steel is taken equal to 200000 MPa, while the Young's modulus of concrete is calculated with the formula provided in Eurocode 2 [12]:

$$E_c = 9500 \cdot \sqrt[3]{f_{cm}}. \tag{7.37}$$

The tensile strength $f_{ct,fl,300}$ is calculated from the flexural strength by applying the size factor proposed by RILEM TC162-TDF [5]:

$$f_{ct,fl,300} = f_{ct,fl} \cdot \frac{1600 - d}{1475}. \tag{7.38}$$

The material properties for all beams are shown in Table 6.

TABLE 6. Material properties for all beams.

Beam	f_{cm}	$f_{ct,fl,300}$	$f_{R,1}$	$f_{R,4}$
	N/mm^2	N/mm^2	N/mm^2	N/mm^2
1	40.2	3.6	0	0
2	40.0	3.5	1.6	1.1
3	38.7	3.9	4.2	3.5
4	40.2	3.6	0	0
5	40.0	3.5	1.6	1.1
6	38.7	3.9	4.2	3.5
7	29.8	3.4	0	0
8	26.8	3.2	1.1	0.8
9	27.5	2.8	2.7	2.1
10	29.8	3.4	0	0
11	26.8	3.2	1.1	0.8
12	27.5	2.8	2.7	2.1
13	48.0	4.7	4.1	3.7
14	46.0	4.5	4.9	2.9
15	50.6	5.0	6.1	3.8
16	47.4	4.4	4.0	3.5
17	40.0	3.5	0	0
18	41.2	4.2	2.3	1.5
19	40.3	4.6	5.9	4.7

7.3. Comparison of experimental and theoretical crack widths

The experimental results as well as the theoretical results calculated with the new RILEM method and with the newly developed physical model are shown in Figs. 25–43.

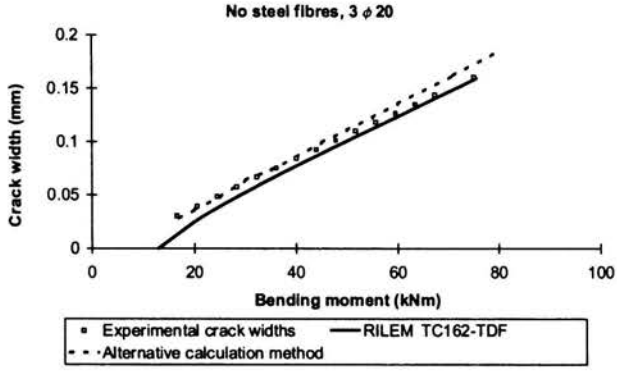

FIGURE 25. Experimental and theoretical crack widths for beam 1.

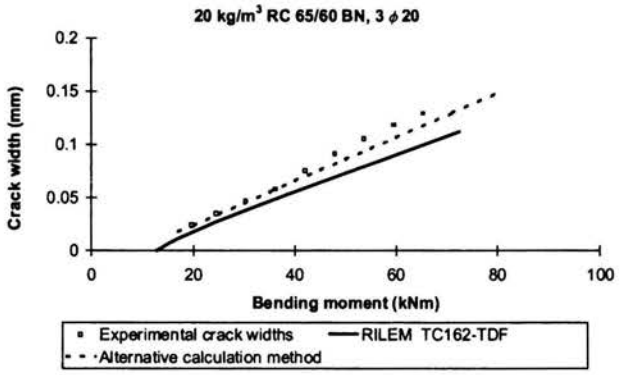

FIGURE 26. Experimental and theoretical crack widths for beam 2.

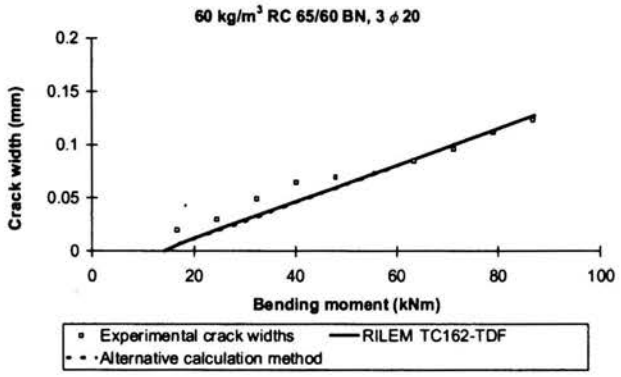

FIGURE 27. Experimental and theoretical crack widths for beam 3.

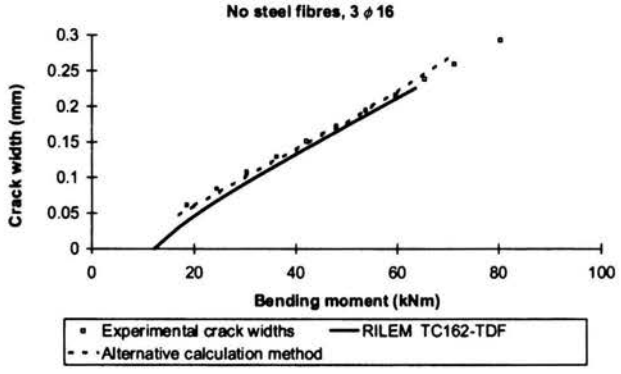

FIGURE 28. Experimental and theoretical crack widths for beam 4.

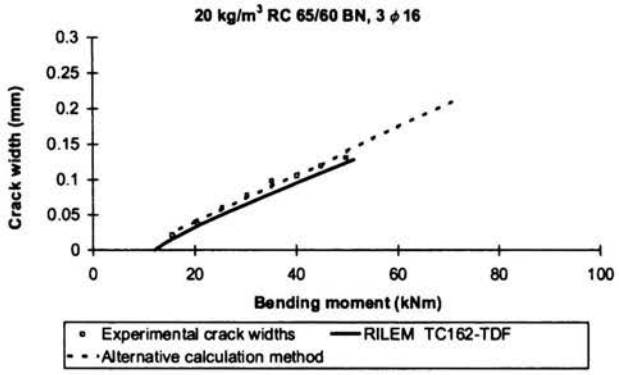

FIGURE 29. Experimental and theoretical crack widths for beam 5.

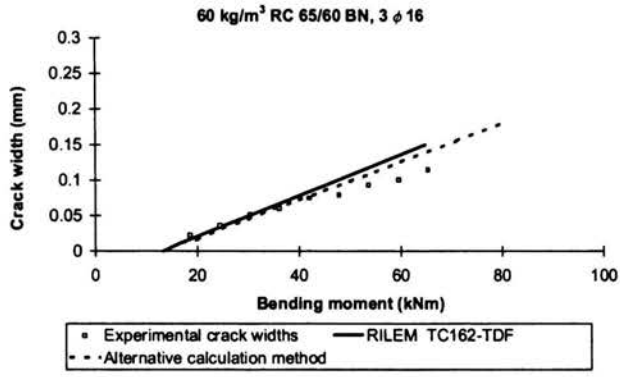

FIGURE 30. Experimental and theoretical crack widths for beam 6.

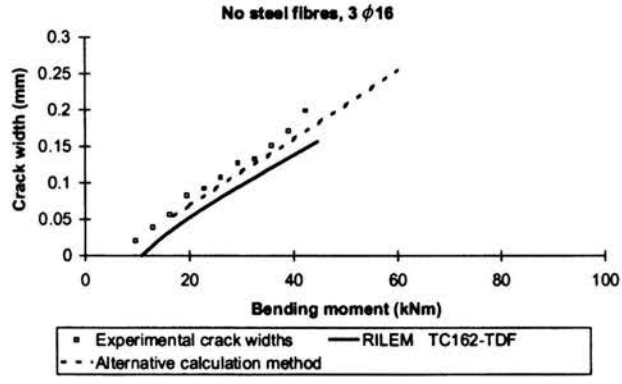

FIGURE 31. Experimental and theoretical crack widths for beam 7.

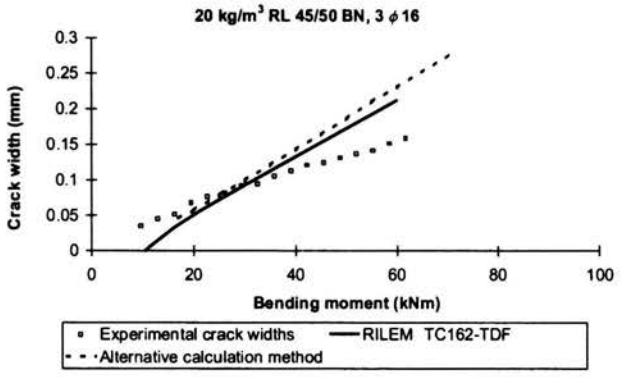

FIGURE 32. Experimental and theoretical crack widths for beam 8.

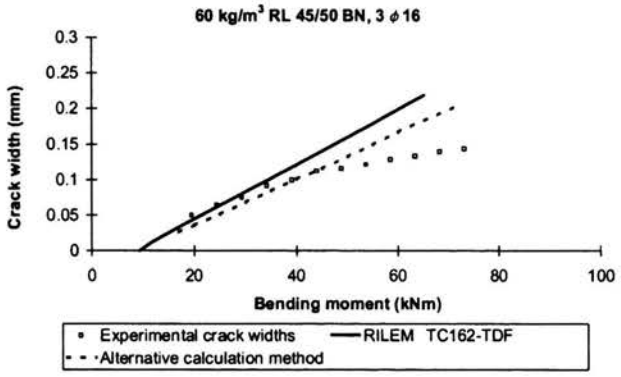

FIGURE 33. Experimental and theoretical crack widths for beam 9.

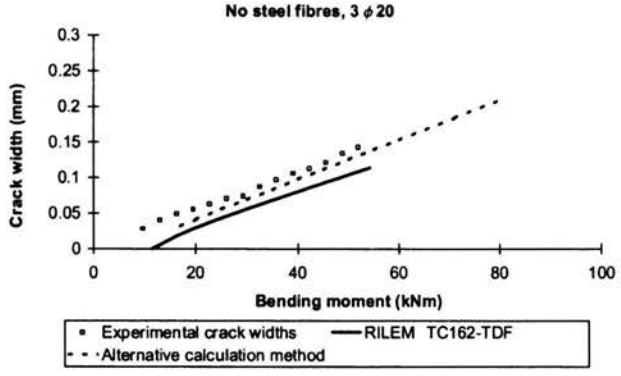

FIGURE 34. Experimental and theoretical crack widths for beam 10.

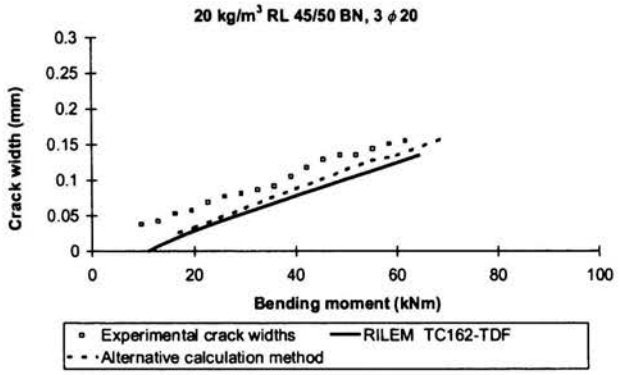

FIGURE 35. Experimental and theoretical crack widths for beam 11.

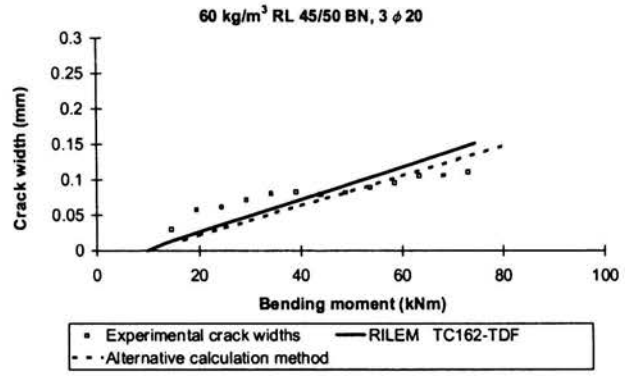

FIGURE 36. Experimental and theoretical crack widths for beam 12.

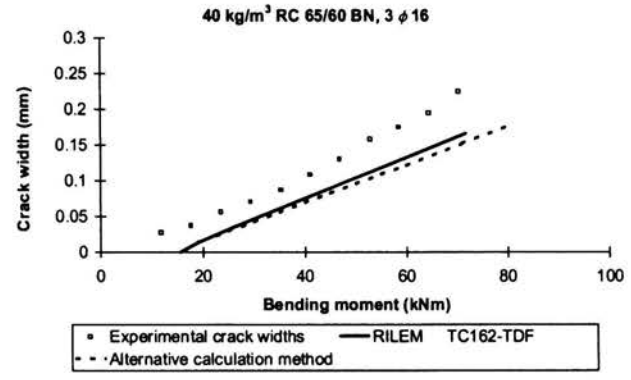

FIGURE 37. Experimental and theoretical crack widths for beam 13.

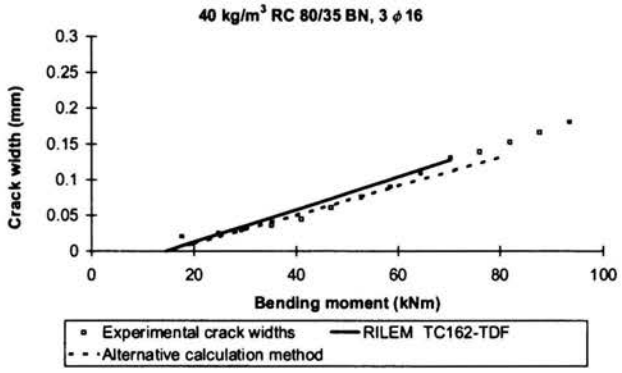

FIGURE 38. Experimental and theoretical crack widths for beam 14.

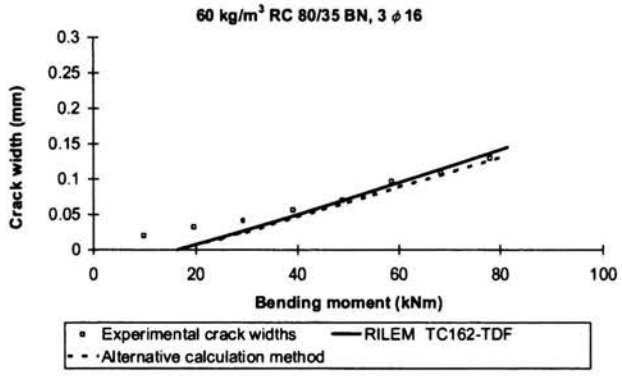

FIGURE 39. Experimental and theoretical crack widths for beam 15.

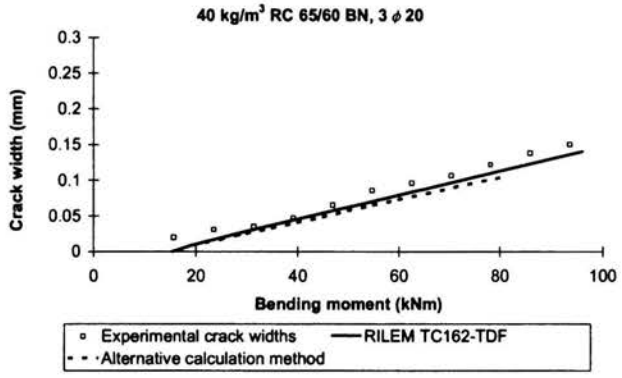

FIGURE 40. Experimental and theoretical crack width for beam 16.

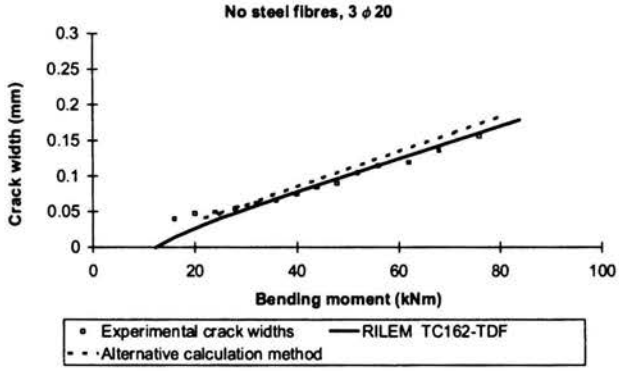

FIGURE 41. Experimental and theoretical crack width for beam 17.

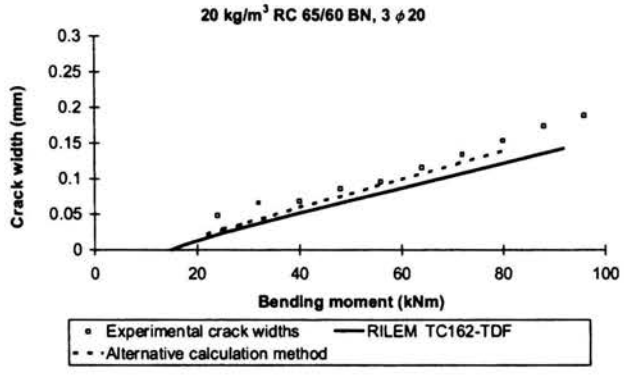

FIGURE 42. Experimental and theoretical crack width for beam 18.

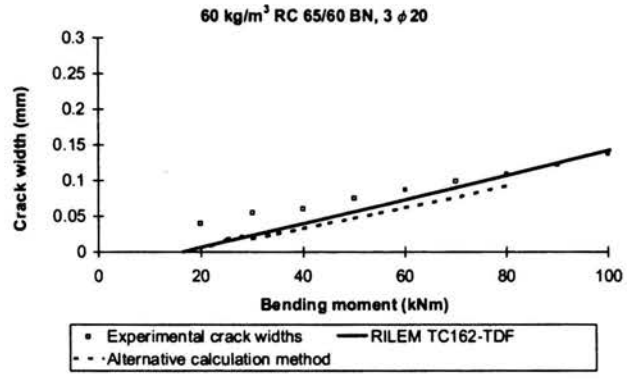

FIGURE 43. Experimental and theoretical crack widths for beam 19.

7.4. Conclusions

A large test program has been executed on 19 full-scale beams. The investigated parameters are the reinforcement ratio, the fibre dosage, the fibre type and the concrete strength. It can be concluded from the test results that steel fibres have a strong beneficial effect on crack widths. For the same amount of longitudinal reinforcement, the addition of 60 kg/m^3 of steel fibres results clearly in a reduction of the crack widths. The benefit of the steel fibres is more obvious for the beams with $3\phi16$ than for the beams with $3\phi20$. This is logical since the portion of the fibres in the total tensile force of the beam is higher in this case.

Two calculation methods have been investigated. The first calculation method is a semi-empirical method which is based on the calculation method of Eurocode 2. The first method is also the new proposal of the RILEM committee TC162-TDF. The second method is quite complicated and based on a physical model. The physical model takes into account the bond between the reinforcement bars and the surrounding concrete as well as the influence of the postcracking tensile strength on the steel strain in a cracked section.

In comparing the calculated crack widths with the experimentally determined crack widths it becomes clear that, taking into account different assumptions as well as the uncertainty on the experimental results, the newly proposed alternative calculation method provides good predictions for all beams. Also the semi-empirical model provides accurate predictions of the crack widths. Since the semi-empirical method is much easier to use and the calculated crack widths are good predictions of the experimental crack widths, this method is by far the most suitable to be used as a standard method for crack width calculation. The newly proposed alternative calculation method on the other hand is rather complicated to use, but in return, it offers a very good insight in the mechanisms that determine the formation of cracks. With the alternative calculation method it becomes possible not only to calculate the crack width, but also the slip at any place between the reinforcement and the surrounding concrete as well as the course of the steel strain along the reinforcement. The physical model provides also the possibility to calculate more complicated structures. In case special types of reinforcement (glass or carbon fibre) are used, this can be taken into account by determining the correct bond stress-slip relation and using the correct Young's modulus.

References

1. D. DUPONT, Modelling and experimental validation of the constitutive law (σ-ε) and cracking behaviour of steel fibre reinforced concrete, *Ph.D.thesis*, K.U.Leuven (Belgium), October 2003.

2. L. VANDEWALLE et al, RILEM TC162-TDF : Test and design methods for steel fibre reinforced concrete - bending test, *Materials and Structures*, Vol.33, January-February, pp.3-5, 2000.

3. L. VANDEWALLE et al, RILEM TC162-TDF : Test and design methods for steel fibre reinforced concrete - bending test (final recommendation), *Materials and Structures*, Vol.35, November, pp.579-582, 2002.

4. L. VANDEWALLE et al, RILEM TC162-TDF : Test and design methods for steel fibre reinforced concrete - σ-ε-design method, *Materials and Structures*, Vol.33, March, pp.75-81, 2000.

5. L. VANDEWALLE et al, RILEM TC162-TDF : Test and design methods for steel fibre reinforced concrete - σ-ε-design method (final recommendation), *Materials and Structures*, Vol.36, October, pp.560-567, 2003.

6. L. VANDEWALLE et al, RILEM TC162-TDF : Test and design methods for steel fibre reinforced concrete - Uni-axial tension test for steel fibre reinforced concrete, *Materials and Structures*, Vol.34, January-February, pp.3-6, 2001.

7. L. VANDEWALLE et al, RILEM TC162-TDF : Test and design methods for steel fibre reinforced concrete - Design of steel fibre reinforced concrete using the σ-w-design method, *Materials and Structures*, Vol.35, June, pp.262-278, 2002.

8. B.I.G. BARR and M.K. LEE, *BRPR-CT98-0813 - Report of Subtask 7.1: Recommendations for Testing of SFRC*, February, ISBN 90-5682-358-2, 2002.

9. B. SCHNÜTGEN and E. ERDEM, *BRPR-CT98-0813 - Report of subtask 4.1: Trial beams in bending and bending and compression*, February, ISBN 90-5682-358-2, 2002.

10. J. ROSENBUSCH and M. TEUTSCH, *BRPR-CT98-0813 - Report of subtask 4.2: Trial beams in shear*, January, ISBN 90-5682-358-2, 2002.

11. Proceedings Workshop *RILEM TC162-TDF: Test and design methods for steel fibre reinforced concrete - Background and experiences*, edited by L.Vandewalle and B.Schnütgen, Rilem Publications S.A.R.L., PRO 31, March 2003.

12. *European pre-standard: ENV 1992-1-1 : Eurocode 2 : Design of Concrete Structures - Part 1 : General rules and rules for buildings*, 1991.

13. B.I.G. BARR, M.K. LEE, E.J. DE PLACE HANSEN, D. DUPONT, E. ERDEM, S. SCHAERLAEKENS, B. SCHNÜTGEN, H. STANG, and L. VANDEWALLE, Round-robin analysis of the RILEM TC162-TDF beam-bending test - Part 1 - Test method evaluation, *Materials and Structures*, Vol.36, November, pp.609-620, 2003.

14. B.I.G. BARR, M.K. LEE, E.J. DE PLACE HANSEN, D. DUPONT, E. ERDEM, S. SCHAERLAEKENS, B. SCHNÜTGEN, H. STANG, and L. VANDEWALLE, Round-robin analysis of the RILEM TC162-TDF beam-bending test - Part 2 -Approximation of δ from the CMOD response, *Materials and Structures*, Vol.36, November, pp.621-630, 2003.

15. B.I.G. BARR, M.K. LEE, E.J. DE PLACE HANSEN, D. DUPONT, E. ERDEM, S. SCHAERLAEKENS, B. SCHNÜTGEN, H. STANG, and L. VANDEWALLE, Round-robin analysis of the RILEM TC162-TDF beam-bending test - Part 3 -Fibre distribution, *Materials and Structures*, Vol.36, November, pp.631-635, 2003.

16. L. VANDEWALLE, *Design with the σ-ε-method*, Proceedings RILEM TC162-TDF Workshop: Test and design methods for steel fibre reinforced concrete – Background and experiences, L.Vandewalle and B.Schnütgen (eds), Rilem Publications S.A.R.L., PRO 31, Bochum, 20-21 March, pp.31-46, 2003.

17. *European pre-standard: ENV 1991-1: Eurocode 1: basis of design and actions on structures - Part 1: Basis of design, Annex D 3.2: Statistical evaluation of resistance/ material tests*, pp.78-80, 1994

18. *European pre-standard: prEN 1992-1 (2^{nd} draft): Eurocode 2: Design of Concrete Structures – Part 1: General rules and rules for buildings*, 2001.

19. L. VANDEWALLE and D. DUPONT, *BRPR-CT98-0813 – Report of subtask 7.2: Recommendations for Design of SFRC*, February, ISBN 90-5682-358-2, 2002.

20. L. VANDEWALLE, Hechting tussen wapening met verbeterde hechting en beton bij gewone en cryogene omstandigheden (in Dutch), *Ph.D.thesis*, K.U.Leuven (Belgium), March 1988.

21. F. DE BONTE, Hechtsterkte bij staalvezelbeton (in Dutch), *Masters thesis*, K.U.Leuven (Belgium), 2000.

22. D. DUPONT, L. VANDEWALLE, and F. DE BONTE, Influence of steel fibres on local bond behaviour, Proceedings of the international symposium *Bond in Concrete – from research to standards*, Budapest, 20-22 November, pp.783-790, 2002.